

THE TRANSIENT ELECTROMAGNETIC FIELD OF A
PULSED LINE SOURCE LOCATED ABOVE A
DISPERSIVELY REFLECTING SURFACE

Scientific Report No. 72

THE TRANSIENT ELECTROMAGNETIC FIELD OF A PULSED LINE
SOURCE LOCATED ABOVE A DISPERSIVELY REFLECTING SURFACE

by

Edward F. Kuester

October 1982

Electromagnetics Laboratory
Department of Electrical Engineering
University of Colorado
Boulder, Colorado 80309

Acknowledgments

A portion of this work was carried out while the author was a visiting scholar at the Laboratory of Electromagnetic Research, Department of Electrical Engineering, Technische Universiteit Delft (TUD), The Netherlands. This work is also partially supported by the U.S. National Science Foundation under Grant No. ECS-801081. A number of helpful discussions with Prof. J. B. Smith, Prof. M. J. Beker and Dr. A. T. Fikri of TUD, and Prof. D. C. Chang of the University of Colorado are gratefully acknowledged.

THE TRANSIENT ELECTROMAGNETIC FIELD OF A
PULSED LINE SOURCE LOCATED ABOVE A
DISPERSIVELY REFLECTING SURFACE

by

Edward F. Kuester
Electromagnetics Laboratory
Department of Electrical Engineering
University of Colorado
Boulder, Colorado 80309

Abstract

An exact representation for the transient field of a pulsed line source above a plane reflecting surface is obtained as a finite integral over the transient plane-wave solution for complex angles of incidence. When applied to the reflection from a conducting half-space, a solution for the transient field is obtained as a finite double integral, which permits accurate calculations in a minimum of computer time. Comparison with early-time and late-time approximations available in the literature shows that there is a wide range of times for which neither is accurate.

Acknowledgments

A portion of this work was carried out while the author was a visiting scientist with the Laboratory of Electromagnetic Research, Department of Electrical Engineering, Technische Hogeschool Delft (THD), The Netherlands. This work is also partially supported by the U.S. National Science Foundation under Grant No. ECS-8021041. A number of helpful discussions with Prof. H. Blok, Prof. A.T. deHoop and Mr. A. Tijhuis of THD, and Prof. D.C. Chang of the University of Colorado are gratefully acknowledged.

1. Introduction

An ability to compute accurately the transient electromagnetic field radiated by pulsed sources in the presence of dispersive media is of great importance in the theory of geophysical prospecting, lightning studies, and development of pulsed antenna systems. At present, even for the simplest of geometries, exact solutions for such problems are not generally available. As a result, one must first solve the corresponding frequency-domain problem (usually expressed as an integral over an infinite interval--a so-called Sommerfeld integral) and then perform another integration over the frequency range $-\infty < \omega < \infty$ or $0 \leq \omega < \infty$ to recover the time-domain solution. It is thus necessary to numerically evaluate a doubly-infinite integral, a process which can be time-consuming and leave uncertain errors in the final results. This has been done for a dipole in a homogeneous half-space in [1], and for a dipole above a two-layer half-space in [2]. Both these works make mention of the numerical difficulties noted above.

Possibly the simplest configuration of all such problems is that of a pulsed line source located above a half-space of frequency-independent conductivity σ and relative permittivity ϵ_r , as shown in Fig. 1. No exact solution of this problem has been given in the literature, to the author's knowledge (short of the formal, doubly-infinite integral referred to before). An approximate, closed-form solution based on Fourier inversion of a "quasi-static" frequency domain expression was obtained in 1930, independently, by Ollendorff [3] and Peterson [4] (a similar solution to a related problem was published many years later by Wait and Hill [5],[6]). By its nature, this solution should be most accurate for large values of time after first arrival of the pulse (wave front). At the other extreme,

the behavior of the fields just after the arrival of the wave front should be governed by the high-frequency part of the frequency-domain solution. In this range, the half-space behaves as a lossless, nondispersive dielectric, and the pulsed line-source problem for this case ($\sigma = 0$) has an exact solution by methods deriving originally from the work of Cagniard [7] and its subsequent development [8]-[11]. There is no indication as to how restricted is the validity of either of these approximations when applied to the general problem of Fig. 1.

Recently [12], a very special problem of this type has been solved in the form of finite double integrals, which considerably facilitates the generation of accurate numerical data. The manner in which this solution was obtained, however, was quite specific to the problem at hand, and it is not clear how the technique might be applied to a more general problem.

A general technique for this class of problems was proposed over 30 years ago in a most regrettably neglected paper by Doak [13]. Unfortunately, since the paper is concerned with three-dimensional geometries, the resulting transformations which occur in the course of his derivation can be hard to follow, and obscure the essentially simple idea of the technique. Moreover, as some of Doak's formal manipulations are invalid in some situations, it is unclear when we may use his results with impunity.

In this paper, we will apply what is, in essence, Doak's method to the two-dimensional problem shown in Fig. 2: a pulsed line source radiating above a fairly arbitrary reflecting boundary. As a specific example, we will present a solution to the arrangement shown in Fig. 1 in the form of a finite double integral. This solution is compared to the approximate (early-time and late-time) solutions referred to above. Along the way, the

physical basis of Doak's method will be set forth, and the subtleties and limitations which are not made clear in [13] will be spelled out.

2. Formulation for an arbitrarily reflecting surface

Let the line source in Fig. 2 carry a current $i(t)$. The corresponding volume current density is $\vec{j}(x,y,t) = \bar{a}_z i(t)\delta(x-2h)\delta(y)$, where \bar{a}_z is the unit vector along the $+z$ -axis. From Maxwell's equations, we find that a TE-polarized field (consisting of the field components e_z , h_x and h_y only) is produced, in which the electric field obeys

$$\left(\nabla_2^2 - \frac{1}{c^2} \frac{\partial^2}{\partial t^2}\right) e_z = \mu_0 i'(t)\delta(x-2h)\delta(y) \quad (1)$$

where $\nabla_2^2 = \partial^2/\partial x^2 + \partial^2/\partial y^2$ is the two-dimensional Laplacian, $c = (\mu_0 \epsilon_0)^{-1/2}$ is the speed of light in vacuo, and ϵ_0, μ_0 are respectively the permittivity and permeability of free space. The \vec{h} -field can also be obtained as the solution of a similar equation. A boundary condition appropriate to the particular surface at $x = h$ must be enforced.

It is customary to solve problems like this one in the frequency domain, and to obtain the time-domain fields by Fourier inversion. To this end, we will introduce a suitable transform pair. We limit consideration to functions of t (i.e., sources and fields) which are causal, that is, which vanish for $t < 0$. For the class of such functions $f(t)$ which are bounded as $t \rightarrow \infty$, we can define the Fourier-Laplace transform $F(\omega)$ as [14]:

$$F(\omega) = \int_0^{\infty} f(t) e^{i\omega t} dt \quad [\text{Im}(\omega) > 0] \quad (2)$$

(the transform of a function denoted by a small letter will be represented by the corresponding capital letter). Then $f(t)$ is expressible by the inversion integral:

$$f(t) = \frac{1}{2\pi} \int_{-\infty+i\delta}^{\infty+i\delta} F(\omega) e^{-i\omega t} d\omega \quad (\delta > 0) \quad (3)$$

From (2) it follows that in the half-plane $\text{Im}(\omega) > 0$, $F(\omega)$ is an analytic function and approaches zero as $|\omega| \rightarrow \infty$. On those occasions when we speak of $F(\omega)$ for real values of ω , we will by implication mean the limit

$$\lim_{\delta \rightarrow 0^+} F(\omega + i\delta)$$

An example of a function which is of special interest to us is the Heaviside unit step-function

$$u(t) = \begin{cases} 0 & t < 0 \\ \frac{1}{2} & t = 0 \\ 1 & t > 0 \end{cases} \quad (4)$$

whose Fourier transform is

$$U(\omega) = \frac{i}{\omega} \quad (5)$$

As is the case here, many Fourier transforms can be analytically continued into the lower half of the ω -plane except for isolated singular points (poles or branch points). The manner in which we carry out this continuation is largely a matter of convenience for the problem at hand.

Applying the Fourier transform to (1), we get

$$(\nabla^2 + k_0^2) E_z = -i\omega\mu_0 I(\omega) \delta(x-2h) \delta(y) \quad (6)$$

where $k_0 = \omega/c$ is the free-space wavenumber. When ω is real and positive, it is customary to determine E_z as a Sommerfeld integral (see, e.g., [10], chapter 5):

$$E_z = \frac{i\omega\mu_0 I(\omega)}{4\pi} \int_{-\infty}^{\infty} \frac{e^{ik_0 \lambda y}}{u_1} \left[e^{-k_0 u_1 |x-2h|} + \Gamma(\lambda, \omega) e^{-k_0 u_1 x} \right] d\lambda \quad (7)$$

($x > h$; ω real, > 0)

where

$$u_1 = (\lambda^2 - 1)^{1/2}; \quad \text{Re}(u_1) \geq 0 \quad (8)$$

The definition of u_1 in (8) specifies a "proper" Riemann sheet in the complex λ -plane, in which the contour of integration in (7) is taken as shown in Fig. 3.

The quantity $\Gamma(\lambda, \omega)$ is the spectral reflection coefficient for a plane wave incident at an angle of $\sin^{-1}(\lambda)$ to the x -axis towards the reflecting surface. The detailed structure of this function depends on the nature of the reflecting surface. In the case of Fig. 1, we have

$$\Gamma(\lambda, \omega) = \frac{u_1 - u_2}{u_1 + u_2} \quad (9)$$

where

$$u_2 = \sqrt{\lambda^2 - n_2^2}; \quad \text{Re}(u_2) \geq 0 \quad (10)$$

and $n_2^2 = \epsilon_r + i/\omega T$, where ϵ_r is the relative permittivity and $T = \epsilon_0/\sigma$ is the conduction relaxation time of the conducting half-space. For a field which satisfies an impedance boundary condition

$$\left. \frac{\partial E_z}{\partial x} \right|_{x=h^+} = i \frac{\omega}{c} Z_s(\omega) E_z \Big|_{x=h^+} \quad (11)$$

involving a dimensionless surface impedance $Z_s(\omega)$, we have

$$\Gamma(\lambda, \omega) = \frac{u_1 - iZ_s(\omega)}{u_1 + iZ_s(\omega)} \quad (12)$$

Other forms for $\Gamma(\lambda, \omega)$ can also be dealt with in the present context.

With ω still restricted to be real and positive, let us consider the reflected portion E_z^r of the field (7), and try to deform the contour of integration in the λ -plane to a special contour $C(\phi)$, shown in Fig. 4.

This contour, known as a Cagniard contour, is such that the term

$ik_0 y - k_0 u_1 x$ in the exponent is always positive imaginary at any point

on $C(\phi)$. In fact, putting

$$\cosh \xi = \lambda \sin \phi + i u_1 \cos \phi \quad (13)$$

we have $i k_0 \lambda y - k_0 u_1 x = i k_0 \rho \cosh \xi$, and further that

$$\left. \begin{aligned} \lambda &= \sin \phi \cosh \xi - i \cos \phi \sinh \xi = -i \sinh(\xi + i\phi) = \sin(\phi = i\xi) \\ u_1 &= \sin \phi \sinh \xi - i \cos \phi \cosh \xi = -i \cosh(\xi + i\phi) = -i \cos(\phi = i\xi) \end{aligned} \right\} \quad (14)$$

which parameterizes $C(\phi)$ when ξ is allowed to vary over $(-\infty, \infty)$. The reflected field will be

$$E_Z^r(x, y; \omega) = \frac{i \omega \mu_0 I(\omega)}{4\pi} \int_{C(\phi)} \frac{e^{i \omega \rho \cosh \xi / c}}{u_1} \Gamma(\lambda, \omega) d\lambda \quad (15)$$

provided that no singularities of $\Gamma(\lambda, \omega)$ in the λ -plane prevent us from deforming the path of integration to $C(\phi)$. For the present, we assume that the deformation is allowed; its validity must be examined in detail for any specific form of $\Gamma(\lambda, \omega)$. Moreover, because the conventional choice for the branch cuts of u_1 as depicted in Figs. 3 and 4 results in part of $C(\phi)$ lying in an "improper" Riemann sheet (see Fig. 4), we shall find it convenient to make an alternate choice for these cuts as shown in Fig. 5. Thus, we take $\text{Im}(u_1) \leq 0$ from here onwards, and we will also choose whatever cuts are present in $\Gamma(\lambda, \omega)$, as a function of λ , so that $C(\phi)$ crosses none of these cuts (if possible). For example, we would take $\text{Im}(u_2) \leq 0$ in (10).

Now, as a function of ω , E_Z^r must be the Fourier-Laplace transform of a causal field $e_Z^r(x, y; t)$, and as such can be continued into the half-plane $\text{Im}(\omega) > 0$ as an analytic function which approaches zero as $|\omega| \rightarrow \infty$ in this half-plane. Now $\exp[i \omega \rho \cosh \xi / c]$ is, for each λ on $C(\phi)$, also such a function of ω , and free from zeroes as well. Since

$I(\omega)$ is arbitrary, but is always analytic and decays as $|\omega| \rightarrow \infty$ in $\text{Im}(\omega) \rightarrow 0$, it seems likely that $\Gamma(\lambda, \omega)$, for each λ on $C(\phi)$, is likewise analytic in $\text{Im}(\omega) > 0$.¹ Hence, the integrand itself of (15) is the frequency response of a causal function of t , and so we can take its inverse Fourier transform first, and integrate the result over $C(\phi)$ afterwards. This interchange of the order of ω - and λ - integrations is the essence of Doak's method.

The result of this interchange is

$$e_z^r(x, y; t) = -\frac{\mu_0}{4\pi} \int_{C(\phi)} e_0(\rho \cosh \xi, \phi - i\xi; t) \frac{d\lambda}{u_1} \quad (16)$$

where

$$e_0(\rho, \phi; t) = \frac{1}{2\pi} \int_{-\infty + i\delta}^{\infty + i\delta} \Gamma(\sin \phi, \omega) [-i\omega I(\omega)] e^{-i\omega(t - \rho/c)} d\omega \quad (17)$$

The quantity $e_0(\rho, \phi; t)$ has the physical significance of being the transient reflected plane wave produced by an incident plane wave of time dependence $i'(t)$ and incidence angle ϕ with respect to the normal ($-x$) direction to the interface. In many specific cases [15]-[22], the reflecting surface is such that e_0 can be evaluated in a convenient form. The present formulation requires an analytic continuation of e_0 to complex values of the angle of incidence ϕ . Since $\Gamma(\lambda, \omega)$ is analytic in $\text{Im}(\omega) > 0$, we can evaluate (17) for $t < \rho/c$ by closing the contour of integration with a semi-circle at infinity in the upper half-plane, so that

$$e_0(\rho, \phi; t) \equiv 0 \quad (t < \rho/c) \quad (18)$$

Hence (16) becomes a finite integral:

¹It should be possible to prove this rigorously, but the author has not succeeded in doing so.

$$e_z^r(x, y; t) = \begin{cases} -\frac{\mu_0}{4\pi} \int_{-\xi_0}^{\xi_0} e_0(\rho \cosh \xi, \phi - i\xi; t) d\xi & (t > \rho/c) \\ 0 & (t < \rho/c) \end{cases} \quad (19)$$

where

$$\xi_0 = \cosh^{-1}\left(\frac{ct}{\rho}\right) = \ln \left[\frac{ct}{\rho} + \sqrt{\left(\frac{ct}{\rho}\right)^2 - 1} \right] \quad (20)$$

The representation (19) is the two-dimensional analog of Doak's result [13], and is equivalent to Filippov's general representation of a solution to the wave equation with a circular wavefront [23].

The plane wave response e_0 can be expressed as the convolution of the current pulse slope $i'(t)$ with the impulse response of the plane wave reflection,

$$e_0(\rho, \phi; t) = \int_{-\infty}^{\infty} i'(t') g(\rho, \phi; t-t') dt' \quad (21)$$

where

$$g(\rho, \phi; t) = \frac{1}{2\pi} \int_{-\infty+i\delta}^{\infty+i\delta} \Gamma(\sin \phi, \omega) e^{-i\omega(t-\rho/c)} d\omega \quad (22)$$

Since e_0 can be recovered from (21) if necessary, we may concentrate on $g(\rho, \phi; t)$ for the remainder of this section.

In most cases, even though it is not a "causal transform" because it does not vanish as $|\omega| \rightarrow \infty$, the reflection coefficient $\Gamma(\lambda, \omega)$ will have a definite high-frequency limiting value $\Gamma_\infty(\lambda)$ as $|\omega| \rightarrow \infty$. In our evaluation of $g(\rho, \phi; t)$, it will be appropriate to split $\Gamma(\lambda, \omega)$ into a "dispersive part" $\Gamma_d(\lambda, \omega)$ which affects mainly the low-frequency components of the reflected wave, and a "specular part" $\Gamma_\infty(\lambda)$ which influences mainly the high-frequency portion of the spectrum:

$$\Gamma(\lambda, \omega) = \Gamma_\infty(\lambda) + \Gamma_d(\lambda, \omega) \quad (23)$$

In most cases it will turn out that $\Gamma_d(\lambda, \omega)$ is $O(\omega^{-1})$ as $|\omega| \rightarrow \infty$. Then the decomposition of g into g_∞ and g_d corresponding to (23) is possible, with g expressed explicitly (in the sense of generalized functions) as

$$g_\infty(\rho, \phi; t) = \frac{1}{2\pi} \Gamma_\infty(\sin \phi) \int_{-\infty}^{\infty} e^{-i\omega(t-\rho/c)} d\omega \quad (24)$$

$$= \Gamma_\infty(\sin \phi) \delta(t - \rho/c)$$

where $\delta(t)$ is the Dirac delta-function. The remaining portion of g is an ordinary function

$$g_d(\rho, \phi; t) = \frac{1}{2\pi} \int_{-\infty+i\delta}^{\infty+i\delta} \Gamma_d(\sin \phi, \omega) e^{-i\omega(t-\rho/c)} d\omega \quad (25)$$

The corresponding decomposition of e_0 is

$$e_0(\rho, \phi; t) = \Gamma_\infty(\sin \phi) i'(t - \rho/c) + \int_{-\infty}^{\infty} i'(t') g_d(\rho, \phi; t-t') dt' \quad (26)$$

Supposing now that $i(t) = I_0 u(t)$ is a step-function, we have

$$e_0(\rho, \phi; t) = \Gamma_\infty(\sin \phi) I_0 \delta(t - \rho/c) + I_0 g_d(\rho, \phi; t) \quad (27)$$

and finally, from (19), we get

$$e_z^r(x, y; t) = - \frac{\mu_0 I_0}{4\pi} \left\{ \frac{\Gamma_\infty[\sin(\phi - i\xi_0)] + \Gamma_\infty[\sin(\phi + i\xi_0)]}{\sqrt{t^2 - \rho^2/c^2}} u(t - \rho/c) \right. \\ \left. + \int_{\xi_0}^{\xi_0} g_d(\rho \cosh \xi, \phi - i\xi; t) d\xi \right\} \quad (28)$$

When the reflecting surface is not dispersive, $\Gamma(\lambda, \omega) = \Gamma_\infty(\lambda)$, $g_d \equiv 0$, and (28) reduces to the form of Cagniard's solution to this problem as given by Felsen [9],[10]. When the dispersive part g_d of the plane-wave impulse response is required, it can often be obtained in closed form, as a series expansion, or as a finite integral [15]-[22]. Thus, we have

reduced the computation of the transient field E_z^r induced by a line source to (at worst) the evaluation of a finite double integral.

3. Fields reflected by a homogeneous conducting half-space

Some of the finer points of this method become clearer when it is applied to a specific configuration. Let us therefore examine the case of a homogeneous, conducting half-space as shown in Fig. 1. In this case, $\Gamma(\lambda, \omega)$ is defined by (9), and has additional (ω -dependent) singularities in the λ -plane at the branch points $\lambda = \pm n_2$ (Fig. 6). As the reader may verify, we appear to have some difficulty when we attempt to deform the contour of integration in the λ -plane to $C(\phi)$, as we have done formally in eqn. (15), if $|\phi| > 45^\circ$. This is because for small enough real values of ω , an additional branch cut integral is obtained around $+n_2$ or $-n_2$ when we attempt the deformation (see Fig. 6). But this is not an essential difficulty if $\epsilon_r > 1$, as we shall now show.

Since $E_z^r(x, y; \omega)$ is the transform of a causal function, we may take its inverse transform not only by integrating (3) just above the real axis of the ω -plane, but also by choosing any path between $-\infty$ and $+\infty$ lying in $\text{Im}(\omega) > 0$. In other words, we may choose δ in (3) to be as large a positive number as we please. Now, we can always choose δ large enough so that for $\omega = \omega_r + i\delta$, $-\infty < \omega_r < +\infty$, the situation shown in Fig. 6 never occurs, and we have instead the situation shown in Fig. 7,² where n_2 always lies to the right, and $-n_2$ always to the left of $C(\phi)$. Because the integrand of (15) is analytic for these values of ω at each λ on $C(\phi)$, the formal manipulations leading to (16) - (28) remain valid provided that

²This is true if $\phi \neq \pm \pi/2$. The extreme cases $\phi = \pi/2$ or $\phi = -\pi/2$ must be treated as limiting cases of our result for $|\phi| < \pi/2$.

we choose δ in (17), (22) and (25) such that the integrands in these expressions are free of singularities in $\text{Im } \omega > \delta$. This requirement has not been made clear in Doak's paper [13].

On the other hand, if $\epsilon_r < 1$, no amount of adjustment to the path of integration in the ω -plane can avoid the necessity of adjoining to $C(\phi)$ an additional branch cut integral around $\pm n_2$ in the λ -plane, if $|\phi|$ is sufficiently large (Fig. 8). We will see later on that even this difficulty is not insurmountable, provided that the path of integration in the ξ -plane in eqn. (28) is moved away from the real axis. That this modification may also need to be made in our formal results is not mentioned in Doak's paper [13] either, and the case when $\epsilon_r < 1$ is simply not treated there.

For the conducting half-space, expressions for the transient reflected plane wave have been derived in [15]-[17]; we include the derivation in Appendix A for completeness. We have

$$\Gamma_\infty(\lambda) = \frac{u_1 - u_r}{u_1 + u_r} \quad (29)$$

where

$$u_r = (\lambda^2 - \epsilon_r)^{1/2} ; \quad \text{Im}(u_r) < 0 \quad \text{on } C(\phi) \quad (30)$$

From (A-5) and (A-6), we have

$$g_d(\rho, \phi; t) = - \frac{u(t-\rho/c)}{\pi T} \frac{\cos \phi}{\sqrt{\epsilon_r - \sin^2 \phi}} \int_0^\pi \frac{\sin^2 \theta \exp \left[- \frac{(t-\rho/c)(1 - \cos \theta)}{2T(\epsilon_r - \sin^2 \phi)} \right]}{(\epsilon_r + 1 - 2 \sin^2 \phi) + (\epsilon_r - 1) \cos \theta} d\theta \quad (31)$$

where the square root is to have positive real part when ϕ is complex.

From (28), we can express the reflected field e_z^r as the sum of a specularly-reflected part $e_{z\infty}^r$ and a dispersive part e_{zd}^r :

$$e_z^r(x, y; t) = e_{z\infty}^r(x, y; t) + e_{zd}^r(x, y; t) \quad (32)$$

The specular part

$$e_{z\infty}^r(x,y;t) = -\frac{\mu_0 I_0}{4\pi} \frac{\{\Gamma_\infty[\sin(\phi - i\xi_0)] + \Gamma_\infty[\sin(\phi + i\xi_0)]\}}{\sqrt{t^2 - \rho^2/c^2}} u(t - \rho/c) \quad (33)$$

$$= \frac{\mu_0 I_0}{2\pi} \frac{u(t - \rho/c)}{\sqrt{t^2 - \rho^2/c^2}} (\epsilon_r - 1) \operatorname{Re} \left\{ \frac{1}{[\cos(\phi - i\xi_0) + \sqrt{\epsilon_r - \sin^2(\phi - i\xi_0)}]^2} \right\} \quad (34)$$

is the "early-time" solution referred to in the Introduction; it dominates e_z^r and becomes singular at the wave front $t = \rho/c$. On the other hand, it decays rather rapidly (as t^{-3}) as $t \rightarrow \infty$. The dispersive part

$$e_{zd}^r(x,y;t) = \frac{\mu_0 I_0 u(t - \rho/c)}{4\pi T} \int_{-\xi_0}^{\xi_0} r(\phi - i\xi; t - \rho \cosh \xi/c) d\xi \quad (35)$$

(where $r(\phi; t)$ is given by (A-6)) vanishes at $t = 0$, but for large t , it only decays as t^{-1} (see Appendix B), and it is appropriate to think of e_{zd}^r as the "late-time" portion of the solution. Since $r(\phi - i\xi; t) = r^*(\phi + i\xi; t)$, with $*$ denoting the complex conjugate, we could also write (35) as

$$e_{zd}^r(x,y;t) = \frac{\mu_0 I_0 u(t - \rho/c)}{2\pi T} \operatorname{Re} \int_0^{\xi_0} r(\phi - i\xi; t - \rho \cosh \xi/c) d\xi \quad (36)$$

which would save some numerical effort in evaluating e_{zd}^r . Since $r(\phi; t)$ is itself given as a finite integral (eqn. (A-6)), we have achieved the reduction of e_z^r to the computation of a finite double integral.

The use of (35) or (36) directly to compute e_{zd}^r can lead to trouble-- a trouble related to the difficulty we had at the beginning of this section in deforming the λ -plane integration contour to $C(\phi)$ when $|\phi| > 45^\circ$.

Inserting (A-6) into (36), we obtain

$$e_{zd}^r(x,y;t) = \frac{\mu_0 I_0 u(t - \rho/c)}{2\pi T} \operatorname{Re} \int_0^{\xi_0} \frac{\cos(\phi - i\xi)}{\sqrt{\epsilon_r - \sin^2(\phi - i\xi)}} \times$$

$$\times \int_0^\pi \frac{\sin^2 \theta \exp \left[-\frac{(t - \rho \cosh \xi/c)(1 - \cos \theta)}{2T(\epsilon_r - \sin^2(\phi - i\xi))} \right]}{(\epsilon_r + 1 - 2 \sin^2(\phi - i\xi)) + (\epsilon_r - 1) \cos \theta} d\theta d\xi$$

Though this expression is apparently cast in a form suitable for direct numerical integration, we find upon examining the integrand of (37) that for large values of t , the exponentiated quantity has positive real part for ξ near ξ_0 and $|\phi| > 45^\circ$. While analytically tolerable, this behavior leads to unacceptable roundoff errors during numerical integration, and thus cannot be used. This trouble can be easily remedied by replacing the ξ -integration by a λ -plane integral once more, and deforming the contour of integration in the λ -plane so that the exponentiated quantity has negative real part and can be integrated numerically without difficulty. One such path is shown in Fig. 9, and consists of a segment of the imaginary axis together with elliptical arcs connecting to the points corresponding to $\xi = \pm \xi_0$. As a result, we can rewrite (35) as:

$$e_{zd}^r(x, y; t) = \frac{\mu_0 I_0 u(t - \rho/c)}{4\pi^2 T} \int_{\lambda_0}^{-\lambda_0^*} \frac{d\lambda}{u_r} \int_0^\pi \frac{\sin^2 \theta \exp \left[\frac{(t - \rho[\lambda \sin \phi + iu_1 \cos \phi]/c)(1 - \cos \theta)}{2Tu_r^2} \right]}{-(u_1^2 + u_r^2) + (\epsilon_r - 1) \cos \theta} d\theta \quad (38)$$

or, more simply as

$$e_{zd}^r(x, y; t) = -\frac{\mu_0 I_0 u(t - \rho/c)}{2\pi^2 T} \operatorname{Re} \int_0^{\lambda_0} \frac{d\lambda}{u_r} \int_0^\pi \frac{\sin^2 \theta \exp \left[\frac{(t - \rho[\lambda \sin \phi + iu_1 \cos \phi]/c)(1 - \cos \theta)}{2Tu_r^2} \right]}{-(u_1^2 + u_r^2) + (\epsilon_r - 1) \cos \theta} d\theta \quad (39)$$

by using the symmetry of the integrand as in (36). Note that this path of integration avoids unnecessarily close encounters with singularities of the integrand, and does not even require modification for the case when $\epsilon_r < 1$. Although the path we have chosen is not unique in its properties, it is probably the simplest to parameterize.

For numerical purposes, it is convenient to break the λ -integration in (39) into an integral along the imaginary axis from 0 to λ_m , where

$$\lambda_m = i \sqrt{\left(\frac{ct}{\rho}\right)^2 - 1} \quad (40)$$

and along the arc from λ_m to λ_0 , with

$$\begin{aligned} \lambda_0 &= \sin \phi \cosh \xi_0 + i \cos \phi \sinh \xi_0 \\ &= \left(\frac{ct}{\rho}\right) \sin \phi + i \cos \phi \sqrt{\left(\frac{ct}{\rho}\right)^2 - 1} \end{aligned} \quad (41)$$

On the vertical part, we introduce a new variable according to $\lambda = is$; on the elliptical arc, we put

$$\lambda = \left(\frac{ct}{\rho}\right) \sin \chi + i \cos \chi \sqrt{\left(\frac{ct}{\rho}\right)^2 - 1}; \quad 0 \leq \chi \leq \phi \quad (42)$$

We now have, in place of (39),

$$\begin{aligned} e_{zd}^r(x, y; t) &= \frac{\mu_0 I_0 u(t - \rho/c)}{2\pi^2 T} \operatorname{Re} \left\{ \int_0^{\sqrt{(ct/\rho)^2 - 1}} \frac{ds}{\sqrt{\epsilon_r + s^2}} \right. \\ &\quad \cdot \int_0^\pi \frac{\sin^2 \theta \exp \left[-\frac{t}{2T} \left(\frac{1 - \cos \theta}{\epsilon_r + s^2} \right) \left(1 - \frac{\rho}{ct} [is \sin \phi + \sqrt{1 + s^2} \cos \phi] \right) \right]}{(\epsilon_r + 1 + 2s^2) + (\epsilon_r - 1) \cos \theta} d\theta \\ &\quad \left. - i \int_0^\phi \frac{g(\chi) d\chi}{\sqrt{g^2(\chi) + \epsilon_r - 1}} \int_0^\pi \frac{\sin^2 \theta \exp \left[-\frac{t}{2T} \left(\frac{1 - \cos(\phi - \chi) - i \sin(\phi - \chi) \sqrt{1 - (\rho/ct)^2}}{g^2(\chi) + \epsilon_r - 1} \right) (1 - \cos \theta) \right]}{2g^2(\chi) + (\epsilon_r - 1)(1 + \cos \theta)} d\theta \right\} \end{aligned} \quad (43)$$

where

$$g(\chi) = \left(\frac{ct}{\rho}\right) \cos \chi - i \sin \chi \sqrt{\left(\frac{ct}{\rho}\right)^2 - 1} \quad (44)$$

and all square roots are to have positive real parts. Expression (43) is now suitable for numerical computation.

4. Numerical results and discussion

We referred in the Introduction to the early-time and late-time solutions available in the literature. The early-time (Cagniard) solution which ignores the effect of conduction currents in the ground is $e_{z\omega}^r$ as given in (34). The late-time solution of Ollendorff and Peterson [3],[4] has been rederived here in Appendix C for convenience, and is given in eqn. (C-9). We will use these two approximate solutions for comparison with the numerically integrated exact solution of eqn. (43).

We first examine a half-space with no dielectric contrast ($\epsilon_r = 1$) but non-zero conductivity. For an observation angle $\phi = 88^\circ$ (close to grazing), the normalized reflected transient field is plotted as a function of t in Figs. 10-12 for three values of normalized radius $\rho/cT = \rho\sigma\zeta_0$, where $\zeta_0 = (\mu_0/\epsilon_0)^{1/2} \approx 377 \Omega$ is the wave impedance of free space. For this case the Cagniard solution is identically zero. The long-time solution begins to become accurate for $t/T \geq 6$ if $\rho/cT \leq 1$, while for larger ρ , we must wait a longer time ($t/T \geq 25$ if $\rho/cT = 5$). Of interest is the fact that the late-time approximation of (C-9) given in (C-10)--a "very-late-time approximation"-- is just as accurate (more so, actually), as the more complicated expression (C-9) when $\rho/cT \leq 1$. Only for large ρ/cT (Fig. 12) is eqn. (C-9) necessary or useful as an approximation to the exact response. In any event, it is a large number of relaxation times before the late-time solution becomes valid.

In Figs. 13-17, we investigate the case $\epsilon_r = 4$ for a succession of observation angles from $\phi = 0^\circ$ to 89.99° . For angles near to grazing (ϕ close to 90°), we begin to observe the effect of the propagation of the wavefront in the half-space (it arrives at $ct/\rho = \sqrt{\epsilon_r} = 2$ when $\phi = 90^\circ$).

When compared to the case $\epsilon_r = 1$, we see that the time when (C-9) becomes accurate is delayed until $t/T \geq 15$ or 20 at $\rho/cT = 1$. It can also be seen that it does not take long ($t/T \approx 1.3$ or 1.4) before the Cagniard solution no longer accurately represents the early portion of the transient response. A large range of t exists when neither approximate solution is accurate and we must use the (numerically) exact solution.

It is especially useful to have an indication of the accuracy of (C-9), which is similar to many such approximations which have been made in geophysical exploration applications. Since these are based upon low-frequency expressions for the field, the best we can usually expect to obtain is an estimate for the accuracy of a "mean-value" or smoothed version of the transient response [27]. For relatively poorly conducting soils where T becomes as large as a microsecond or so, we have seen that our more precise evaluation of the transient field shows an important range where (C-9) cannot be used. When current pulses with duration of a few T are used, such approximations become almost unusable.

5. Conclusion

We have given a two-dimensional version of Doak's [13] method for computing transient reflected fields from a plane surface. The method is applied to reflection from a conducting half-space, providing an efficient and accurate computational procedure.

Since Doak's method is applied to three-dimensional problems in [13], it seems clear that the procedure used here is susceptible to generalization in several directions. These generalizations will provide a fruitful area for future research. In particular, the other (TM) polarization of fields above a conducting half-space displays the effect of the so-called

ground wave in the frequency domain. Although it is known [12] that no wavefront is associated with this ground wave, it seems plausible that it will exert a substantial influence on the transient field near the interface. This problem will be the subject of a future investigation.

Of a more fundamental nature is the restriction that our observation point and source point both lie in the air region. Buried sources and observers are of considerable interest in geophysical applications; however, the λ -plane contour $C(\phi)$ as we have used here will not serve its intended purpose if source or observation point is buried. It would be highly important if this difficulty could be overcome. This problem is currently under study as well.

It might also be mentioned in closing that more complicated dispersion models for the half-space may be desirable in certain applications. Certain of these have been suggested, e.g., in [1]. These could be included in the present framework so long as a suitable finite integral solution could be found for the transient reflected plane wave $e_0(\rho, \phi; t)$. This is likely to be the case provided the dispersion model is not too complicated.

References

- [1] J.A. Fuller and J.R. Wait, "A pulsed dipole in the earth," in Transient Electromagnetic Fields (L.B. Felsen, ed.). Berlin: Springer-Verlag, 1976, pp. 237-269.
- [2] A. Ezzeddine, J.A. Kong and L. Tsang, "Time response of a vertical electric dipole over a two-layer medium by the double deformation technique," J. Appl. Phys. vol. 53, pp. 813-822 (1982).
- [3] F. Ollendorff, "Die Schwachstrombeeinflussung durch plötzlich geschaltete Erdstromfelder," Elektr. Nachr.-Technik vol. 7, pp. 393-407 (1930).
- [4] L.C. Peterson, "Transients in grounded circuits, one of which is of infinite length," Bell Syst. Tech. J. vol. 9, pp. 760-769 (1930).
- [5] J.R. Wait, "Transient excitation of the earth by a line source of current," Proc. IEEE vol. 59, pp. 1287-1288 (1971).
- [6] D.A. Hill and J.R. Wait, "Diffusion of electromagnetic pulses into the earth from a line source," IEEE Trans. Ant. Prop. vol. 22, pp. 145-146 (1974).
- [7] L. Cagniard, Reflection and Refraction of Progressive Seismic Waves (E.A. Flinn and C.H. Dix, eds.). New York: McGraw-Hill, 1962.
- [8] A.T. deHoop, "A modification of Cagniard's method for solving seismic pulse problems," Appl. Sci. Res. vol. B8, pp. 349-356 (1960).
- [9] L.B. Felsen, "Transient solutions for a class of diffraction problems," Quart. Appl. Math. vol. 23, pp. 151-169 (1965).
- [10] L.B. Felsen and N. Marcuvitz, Radiation and Scattering of Waves. Englewood Cliffs, NJ: Prentice-Hall, 1973, pp. 116-117, 450-452, 523-529.
- [11] A.T. DeHoop, "Pulsed electromagnetic radiation from a line source in a two-media configuration," Radio Science, vol. 14, pp. 253-268 (1979).
- [12] H. Haddad and D.C. Chang, "Transient electromagnetic field generated by a vertical electric dipole on the surface of a dissipative earth," Radio Science vol. 16, pp. 169-177 (1981).
- [13] P.E. Doak, "The reflexion of a spherical acoustic pulse by an absorbent infinite plane and related problems," Proc. Roy. Soc. (London), vol. A215, pp. 233-254 (1952).
- [14] B. Davies, Integral Transforms and their Applications. New York: Springer-Verlag, 1978, pp. 1-25, 89-109.

- [15] J.R. Wait and C. Froese, "Reflection of a transient electromagnetic wave at a conducting surface," J. Geophys. Res. vol. 60, pp. 97-103 (1955).
- [16] Yu. A. Medvedev, "Reflection of an electromagnetic pulse from the planar boundary of an absorber [Russian]," Izv. VUZ Radiofizika vol. 11, pp. 1528-1532 (1968) [Engl. transl. in Radiophys. Quantum Electron. vol. 11, pp. 860-862 (1968).
- [17] D.G. Dudley, T.M. Papazoglou and R.C. White, "On the interaction of a transient electromagnetic plane wave and a lossy half-space," J. Appl. Phys. vol. 45, pp. 1171-1175 (1974).
- [18] J.R. Wait, "Reflection of a plane transient electromagnetic wave from a cold lossless plasma slab," Radio Science vol. 4, pp. 401-405 (1969).
- [19] J.R. Wait, "Oblique reflection of a plane impulsive electromagnetic wave from a plasma half-space," Phys. Fluids vol. 12, pp. 1521-1522 (1969).
- [20] J.R. Wait, "On the reflection of electromagnetic pulses from the ionosphere," Radio Science vol. 5, pp. 1461-1467 (1970).
- [21] D.M. Chabries and D.M. Bolle, "Impulse reflection with arbitrary angle of incidence and polarization from isotropic plasma slabs," Radio Science vol. 6, pp. 1143-1149 (1971).
- [22] W.M. Boerner and Y.M. Antar, "Aspects of electromagnetic pulse scattering from a grounded dielectric slab," Arch. Elek. Übertragungstech. vol. 26, pp. 14-21 (1972).
- [23] A.F. Filippov, "Integral representations of solutions of the two-dimensional wave equation and diffraction problems [Russian]," Zh. Vychisl. Mat. Mat. Fiz. vol. 17, pp. 718-728 (1977) [Engl. trans. in USSR Comp. Math. Math. Phys. vol. 17, no. 3, pp. 153-163 (1977)].
- [24] I.S. Gradshteyn and I.M. Ryzhik, Table of Integrals, Series, and Products. New York: Academic Press, 1965.
- [25] M. Abramowitz and I.A. Stegun (eds.), Handbook of Mathematical Functions. Washington, DC: U.S. Government Printing Office, 1964.
- [26] F. Oberhettinger and L. Badii, Tables of Laplace Transforms. New York: Springer-Verlag, 1973.
- [27] H.G. Baerwald, "Some relations between transient phenomena in systems with similar frequency characteristics," Phil. Mag. ser. 7, vol. 21, pp. 833-869 (1936).

APPENDIX A

Evaluation of $g_d(\rho, \phi; t)$ for a conducting half-space

In this appendix, we will derive a finite integral expression for $g_d(\rho, \phi; t)$ as defined by (25) in the case when $\Gamma(\lambda, \omega)$ is given by (9). Some important properties of g_d will also be given.

Evidently, we have

$$\Gamma_\infty(\lambda) = \frac{u_1 - u_r}{u_1 + u_r} \quad (A-1)$$

where

$$u_r = (\lambda^2 - \epsilon_r)^{1/2}; \quad \text{Im}(u_r) < 0 \quad (A-2)$$

so that

$$\begin{aligned} \Gamma_d(\lambda, \omega) &= \frac{u_1 - u_2}{u_1 + u_2} - \frac{u_1 - u_r}{u_1 + u_r} \\ &= \frac{f(\lambda) - \sqrt{1 - \frac{i}{\omega T u_r^2}}}{f(\lambda) + \sqrt{1 - \frac{i}{\omega T u_r^2}}} - \frac{f(\lambda) - 1}{f(\lambda) + 1} \end{aligned} \quad (A-3)$$

where $f(\lambda) = u_1/u_r$. For fixed λ on $C(\phi)$, we define a branch cut in the ω -plane between $\omega=0$ and $\omega = i/Tu_r^2$ as shown in Fig. A.1. Note that i/Tu_r^2 may lie above the real axis, and δ should be chosen sufficiently large that the inversion contour in (25) is above this singularity. We now evaluate g_d from (25) by closing the integration contour with a semicircle at ∞ in either the upper or lower half-plane, according to whether $t < \rho/c$ or $t > \rho/c$ respectively. Since

$$\Gamma_d(\lambda, \omega) = O(1/\omega)$$

as $|\omega| \rightarrow \infty$, and the integrand is analytic for $\text{Im}(\omega) > \delta$, we have

$$g_d(\rho, \phi; t) = 0 \quad (t < \rho/c) \quad (A-4)$$

On the other hand, there is no residue contribution at either of the branch points, and the apparent pole of (A-3) located at $\omega = -i/T(\epsilon_r - 1)$ does not lie on the Riemann sheet specified in Fig. A.1. Hence, for $t > \rho/c$, g_d can be written as a branch cut integral. Making the change of variable

$$\omega = \frac{i}{2u_r^2 T} (1 - \cos \theta)$$

in this integral, and combining the result with (A-4), we obtain

$$g_d(\rho, \phi; t) = -u(t - \rho/c) \frac{r(\phi; t - \rho/c)}{T} \quad (A-5)$$

where

$$r(\phi; t) = \frac{\cos \phi}{\pi \sqrt{\epsilon_r - \sin^2 \phi}} \int_0^\pi \frac{\sin^2 \theta \exp \left[-\frac{t(1 - \cos \theta)}{2T(\epsilon_r - \sin^2 \phi)} \right]}{(\epsilon_r + 1 - 2 \sin^2 \phi) + (\epsilon_r - 1) \cos \theta} d\theta \quad (A-6)$$

The remaining square root in (A-6) is to have positive real part when ϕ is complex.

Though $r(\phi; t)$ is not expressible in finite form using the standard special functions, we can evaluate it both for $t=0$ and as $t \rightarrow \infty$. At $t=0$, we make use of [24], formula 3.644.4 to obtain

$$r(\phi; 0) = \frac{\cos \phi}{\sqrt{\epsilon_r - \sin^2 \phi}} \frac{1}{(\cos \phi + \sqrt{\epsilon_r - \sin^2 \phi})^2} \quad (A-7)$$

On the other hand put $x = (1 - \cos \theta)/2$, and let $\tau = t/T(\epsilon_r - \sin^2 \phi)$ to get

$$r(\phi; t) = \frac{2}{\pi} \frac{\cos \phi}{\sqrt{\epsilon_r - \sin^2 \phi}} \int_0^1 \frac{\sqrt{x(1-x)} e^{-\tau x} dx}{(\epsilon_r - \sin^2 \phi) - (\epsilon_r - 1)x} \quad (A-8)$$

If $\text{Re}(\tau) > 0$ and $|\tau(\epsilon_r - \sin^2 \phi)/(\epsilon_r - 1)| = t/T(\epsilon_r - 1) \gg 1$ and $|\tau| \gg 1$, we have by standard asymptotic techniques that

$$\begin{aligned}
 r(\phi; t) &\sim \frac{2}{\pi} \frac{\cos \phi}{\sqrt{\epsilon_r - \sin^2 \phi}} \int_0^\infty \frac{\sqrt{x} e^{-Tx} dx}{\epsilon_r - \sin^2 \phi} \\
 &= \frac{\cos \phi}{\sqrt{\pi}} (t/T)^{-3/2} \quad (t \rightarrow \infty)
 \end{aligned}
 \tag{A-9}$$

In the special case $\epsilon_r = 1$, (A-6) reduces to a known integral representation of a modified Bessel function ([25], p. 376):

$$r(\phi; t) = \frac{T}{t} e^{-\frac{t}{2T \cos^2 \phi}} I_1\left(\frac{t}{2T \cos^2 \phi}\right) \quad (\epsilon_r = 1) \tag{A-10}$$

It can be checked that (A-10) agrees with (A-7) and (A-9) in the appropriate limits, if we put $\epsilon_r = 1$ therein.

APPENDIX B

Approximation of e_{zd}^r for $ct/\rho \approx 1$ and $t \rightarrow \infty$

In this appendix, we obtain the limiting forms for e_{zd}^r near the wavefront ($ct/\rho \approx 1$) and for very long times ($t \rightarrow \infty$).

For $ct/\rho \approx 1$, we have $\xi_0 \approx \sqrt{2(ct/\rho - 1)} \ll 1$, and from (36),

$$\begin{aligned} e_{zd}^r(x, y; t) &\approx \frac{\mu_0 I_0 u(t - \rho/c)}{2\pi T} \operatorname{Re} \left\{ \sqrt{2(ct/\rho - 1)} r(\phi; 0) \right\} \\ &= \frac{\mu_0 I_0}{\pi T} \sqrt{\frac{ct/\rho - 1}{2}} \frac{\cos \phi}{\sqrt{\epsilon_r - \sin^2 \phi}} \cdot \frac{1}{(\cos \phi + \sqrt{\epsilon_r - \sin^2 \phi})^2}; \\ &\quad (ct \approx \rho) \end{aligned} \quad (B-1)$$

where we have used the result (A-7). Clearly, e_{zd}^r vanishes at $t = \rho/c$.

When $t \rightarrow \infty$, it is most convenient to start from (43). Let us first assume that $ct/\rho \gg 1$ and $ct/\rho \gg \sqrt{\epsilon_r}$. The second term in curly brackets in (43) is approximately given by

$$-i\left(\frac{\rho}{ct}\right)^2 \int_0^\phi d\chi \int_0^\pi e^{i2\chi} \sin^2 \theta \exp\left[-\frac{t}{2T}\left(\frac{\rho}{ct}\right)^2 (1 - \cos \theta) (e^{2i\chi} - e^{i(\phi+\chi)})\right] d\theta \quad (B-2)$$

If, further, t is large enough that $(\rho/ct)(\rho/ct) \ll 1$, then (B-2) is approximately

$$-i\left(\frac{\rho}{ct}\right)^2 \int_0^\phi d\chi \int_0^\pi e^{i2\chi} \sin^2 \theta d\theta = \frac{\pi(\rho/ct)^2}{4} (1 - e^{2i\phi}) \quad (B-3)$$

The first integral in the curly brackets of (43) owes most of its value to the range of s where $s \gg 1$ and $s \gg \sqrt{\epsilon_r}$. Following standard asymptotic arguments, it is given approximately for $ct/\rho \gg 1$ and $ct/\rho \gg \sqrt{\epsilon_r}$ as

$$\frac{1}{2} \int_0^{ct/\rho} \frac{ds}{s^3} \int_0^\pi \sin^2 \theta \exp\left[-\frac{t}{2T}(1 - \cos \theta) \left(\frac{1}{s^2} - \frac{\rho}{cts} e^{i\phi}\right)\right] d\theta \quad (B-4)$$

We make the change of variable $v = ct/\rho s - 1$ in (B-4) to get

$$\frac{1}{2} \left(\frac{\rho}{ct} \right)^2 \int_0^\infty (v+1) dv \int_0^\pi \sin^2 \theta \exp \left[-\frac{1}{2} \left(\frac{\rho}{ct} \right) \left(\frac{\rho}{ct} \right) ((v+1)^2 - (v+1) e^{i\phi}) (1 - \cos \theta) \right] d\theta \quad (B-5)$$

Using a result from [25], p. 302, the v -integral can be evaluated, and (B-5) becomes

$$\begin{aligned} & \frac{T}{2t} \int_0^\pi (1 + \cos \theta) \left\{ \exp \left[-\frac{1}{2} \left(\frac{\rho}{ct} \right) \left(\frac{\rho}{ct} \right) (1 - e^{i\phi}) (1 - \cos \theta) \right] \right. \\ & + \frac{e^{i\phi}}{2} \sqrt{\frac{\pi}{2} \left(\frac{\rho}{ct} \right) \left(\frac{\rho}{ct} \right) (1 - \cos \theta)} \exp \left[\frac{3}{2} \left(\frac{\rho}{ct} \right) \left(\frac{\rho}{ct} \right) (1 - e^{i\phi}) (1 - \cos \theta) \right] \cdot \\ & \left. \cdot \operatorname{erfc} \left[(2 - e^{i\phi}) \sqrt{\frac{\pi}{2} \left(\frac{\rho}{ct} \right) \left(\frac{\rho}{ct} \right) (1 - \cos \theta)} \right] \right\} d\theta \end{aligned} \quad (B-6)$$

where $\operatorname{erfc}(z)$ is the complementary error function ([25], p. 297). If now $(\rho/ct)(\rho/ct) \ll 1$, then (B-6) reduces to

$$\begin{aligned} & \frac{T}{2t} \int_0^\pi (1 + \cos \theta) \left[1 + \frac{e^{i\phi}}{2} \sqrt{\frac{\pi}{2} \left(\frac{\rho}{ct} \right) \left(\frac{\rho}{ct} \right)} (1 - \cos \theta)^{1/2} + O(t^{-1}) \right] d\theta \\ & = \frac{\pi T}{2t} + \frac{e^{i\phi}}{3} \frac{\rho \sqrt{\pi T}}{ct^{3/2}} + O(t^{-2}) \end{aligned} \quad (B-7)$$

Combining (B-3) and (B-7) with (43), we find that

$$e_{zd}^r(x, y; t) \approx \frac{\mu_0 I_0}{4\pi} \left\{ \frac{1}{t} + \frac{2}{3} \frac{\rho}{c\sqrt{\pi T}} \frac{\cos \phi}{t^{3/2}} + O(t^{-2}) \right\}; \quad (t \rightarrow \infty) \quad (B-8)$$

APPENDIX C

The "quasistatic" transient response of a line source above a conducting half-space

In this appendix we present a derivation for the "quasistatic" (long-time) response to a pulsed line-source above a homogeneous, conducting half-space. The result is identical to those of [3] and [4], although the method of derivation is rather different. Related quasistatic solutions for a buried line source have been given in [5] and [6], whose analyses are mathematically equivalent to portions of those in [3].

From (7) and (9), the reflected field in the frequency-domain for the case of a step-function current pulse

$$i(t) = I_0 u(t) \quad (C-1)$$

is

$$E_z^r(x, y; \omega) = E_{zc}^r(x, y; \omega) + E_{zf}^r(x, y; \omega) \quad (C-2)$$

where E_{zc}^r is the field which would be reflected from a perfect conductor at $s = h$:

$$\begin{aligned} E_{zc}^r(x, y; \omega) &= \frac{\mu_0 I_0}{4\pi} \int_{-\infty}^{\infty} \frac{e^{ik_0 \lambda y - k_0 u_1 x}}{u_1} d\lambda \\ &= \frac{i\mu_0 I_0}{4} H_0^{(1)}\left(\frac{\omega \rho}{c}\right) \end{aligned} \quad (C-3)$$

while E_{zf}^r is a correction term attributable to the finite conductivity of the half-space:

$$E_{zf}^r(x, y; \omega) = -\frac{\mu_0 I_0}{2\pi} \int_{-\infty}^{\infty} \frac{e^{ik_0 \lambda y - k_0 u_1 x}}{u_1 + u_2} d\lambda \quad (C-4)$$

In (C-3), $H_0^{(1)}$ is a Hankel function of the first kind.

The transient response corresponding to (C-3) can be found if we first analytically continue this function in to the complex ω -plane so that it has

no singularities for $\text{Im}(\omega) > 0$. A convenient way of doing this is according to the branch cut shown in Fig. C.1. In the usual fashion, we find e_{zc}^r for $t < \rho/c$ by closing the contour at infinity in the upper half-plane, and for $t > \rho/c$ by closing in the lower half-plane (picking up a branch-cut integral). Using the continuation relations for Bessel functions, and their connection with modified Bessel functions, we find that

$$\begin{aligned} e_{zc}^r(x, y; t) &= \frac{i\mu_0 I_0}{8\pi} \int_{-\infty + i\delta}^{\infty + i\delta} e^{-i\omega t} H_0^{(1)}\left(\omega \frac{\rho}{c}\right) d\omega \\ &= \left\{ \frac{\mu_0 I_0}{2\pi} \int_0^{\infty} e^{-st} I_0\left(\frac{s\rho}{c}\right) ds \right\} u(t - \rho/c) \\ &= \frac{\mu_0 I_0 u(t - \rho/c)}{2\pi\sqrt{t^2 - \rho^2/c^2}} \end{aligned} \quad (C-5)$$

where $I_0(z)$ is a modified Bessel function of the first kind (not to be confused with the current I_0) and formula 6.611.4 of [24] has been used.

In the quasistatic limit, (C-4) is treated approximately by making the change of variable $\lambda = v/\sqrt{\omega T}$, and neglecting the quantity ωT compared to v^2 and to $(v^2 - i)/\epsilon_r$:

$$E_{zf}^r(x, y; \omega) \approx - \frac{\mu_0 I_0}{\pi} \int_0^{\infty} \cos\left(\frac{vy}{c} \sqrt{\frac{\omega}{T}}\right) e^{-\frac{vx}{c} \sqrt{\frac{\omega}{T}}} \frac{dv}{v + \sqrt{v^2 - i}} \quad (C-6)$$

In order for (C-6) to be valid, we must also assume that $(\rho/c)\sqrt{\omega/T}$ is not too large, i.e., that $\sqrt{\omega T}$ is small compared to cT/ρ . If the cosine in (C-6) is expressed as the sum of two exponentials, we may obtain the integral in terms of Struve and Neumann functions ([24], formula 3.368):

$$\begin{aligned} E_{zf}^r(x, y; \omega) \approx & - \frac{\mu_0 I_0}{2\pi} \left\{ \frac{\pi c}{2\rho} \sqrt{\frac{T}{\omega}} e^{\pi i/4} \left[e^{-i\phi} \left\{ H_1\left[\frac{\rho}{c} \sqrt{\frac{\omega}{T}} e^{i(\phi - \frac{\pi}{4})}\right] - Y_1\left[\frac{\rho}{c} \sqrt{\frac{\omega}{T}} e^{i(\phi - \frac{\pi}{4})}\right] \right\} \right. \right. \\ & + e^{i\phi} \left\{ H_1\left[\frac{\rho}{c} \sqrt{\frac{\omega}{T}} e^{-i(\phi + \frac{\pi}{4})}\right] - Y_1\left[\frac{\rho}{c} \sqrt{\frac{\omega}{T}} e^{-i(\phi + \frac{\pi}{4})}\right] \right\} \\ & \left. \left. - 2i \frac{c^2}{\rho^2} \frac{T}{\omega} \cos 2\phi \right\} \right\} \end{aligned} \quad (C-7)$$

no singularities for $\text{Im}(\omega) > 0$. A convenient way of doing this is according to the branch cut shown in Fig. C.1. In the usual fashion, we find e_{zc}^r for $t < \rho/c$ by closing the contour at infinity in the upper half-plane, and for $t > \rho/c$ by closing in the lower half-plane (picking up a branch-cut integral). Using the continuation relations for Bessel functions, and their connection with modified Bessel functions, we find that

$$\begin{aligned} e_{zc}^r(x, y; t) &= \frac{i\mu_0 I_0}{8\pi} \int_{-\infty + i\delta}^{\infty + i\delta} e^{-i\omega t} H_0^{(1)}\left(\omega \frac{\rho}{c}\right) d\omega \\ &= \left\{ \frac{\mu_0 I_0}{2\pi} \int_0^{\infty} e^{-st} I_0\left(\frac{s\rho}{c}\right) ds \right\} u(t - \rho/c) \\ &= \frac{\mu_0 I_0 u(t - \rho/c)}{2\pi \sqrt{t^2 - \rho^2/c^2}} \end{aligned} \quad (C-5)$$

where $I_0(z)$ is a modified Bessel function of the first kind (not to be confused with the current I_0) and formula 6.611.4 of [24] has been used.

In the quasistatic limit, (C-4) is treated approximately by making the change of variable $\lambda = v/\sqrt{\omega T}$, and neglecting the quantity ωT compared to v^2 and to $(v^2 - i)/\epsilon_r$:

$$E_{zf}^r(x, y; \omega) \approx -\frac{\mu_0 I_0}{\pi} \int_0^{\infty} \cos\left(\frac{vy}{c} \sqrt{\frac{\omega}{T}}\right) e^{-\frac{vx}{c} \sqrt{\frac{\omega}{T}}} \frac{dv}{v + \sqrt{v^2 - i}} \quad (C-6)$$

In order for (C-6) to be valid, we must also assume that $(\rho/c)\sqrt{\omega/T}$ is not too large, i.e., that $\sqrt{\omega T}$ is small compared to cT/ρ . If the cosine in (C-6) is expressed as the sum of two exponentials, we may obtain the integral in terms of Struve and Neumann functions ([24], formula 3.368):

$$\begin{aligned} E_{zf}^r(x, y; \omega) \approx & -\frac{\mu_0 I_0}{2\pi} \left\{ \frac{\pi c}{2\rho} \sqrt{\frac{T}{\omega}} e^{\pi i/4} \left[e^{-i\phi} \left\{ H_1\left[\frac{\rho}{c} \sqrt{\frac{\omega}{T}}\right] e^{i(\phi - \frac{\pi}{4})} - Y_1\left[\frac{\rho}{c} \sqrt{\frac{\omega}{T}}\right] e^{i(\phi - \frac{\pi}{4})} \right\} \right. \right. \\ & + e^{i\phi} \left\{ H_1\left[\frac{\rho}{c} \sqrt{\frac{\omega}{T}}\right] e^{-i(\phi + \frac{\pi}{4})} - Y_1\left[\frac{\rho}{c} \sqrt{\frac{\omega}{T}}\right] e^{-i(\phi + \frac{\pi}{4})} \right\} \left. \right] \\ & - 2i \frac{c^2}{\rho^2} \frac{T}{\omega} \cos 2\phi \left. \right\} \end{aligned} \quad (C-7)$$

where H_1 and Y_1 are respectively the Struve and Neumann functions of order one. The corresponding time-domain function may be evaluated using contour deformation in the ω -plane after analytically continuing (C-7) into the same cut plane in Fig. C.1. However, because of the asymptotic behavior of (C-7) as $|\omega| \rightarrow \infty$ we close in the upper half-plane for $t < 0$ (obtaining a zero result), and in the lower half-plane for $t > 0$, wrapping the contour around the branch cut. This means that our approximation to e_{zf}^r has an "arrival time" of $t = 0$; the quasistatic approximation gives a signal with no propagation delay. However, we can only expect that an approximation of E_{zf}^r for small ω will result in an approximation of e_{zf}^r valid for sufficiently large values of t , so this early arrival can be ignored. Upon performing the indicated operations, we obtain

$$\begin{aligned} e_{zf}^r(x,y;t) &\approx -\frac{\mu_0 I_0}{2\pi} \frac{c\sqrt{t}}{\rho} u(t) \operatorname{Re} \left\{ e^{-i\phi} \int_0^\infty e^{-st} \left[H_1 \left(\frac{-i\rho e^{i\phi}}{c\sqrt{t}} \sqrt{s} \right) + iJ_1 \left(\frac{-i\rho e^{i\phi}}{c\sqrt{t}} \sqrt{s} \right) \right] \frac{ds}{\sqrt{s}} \right\} \\ &= \frac{\mu_0 I_0}{\pi} \frac{c\sqrt{t}}{\rho} u(t) \operatorname{Re} \left\{ -\frac{e^{-i\phi}}{(\pi t)^{1/2}} + \frac{c\sqrt{t}}{\rho} e^{-2i\phi} \left[1 - w \left(\frac{i\rho e^{i\phi}}{2c\sqrt{t}t} \right) \right] \right\} \quad (C-8) \end{aligned}$$

We have used formulas 16.27 and 14.23 of [26], and introduced the function ([25], p. 297):

$$w(z) = e^{-z^2} \operatorname{erfc}(-iz)$$

where erfc is the complementary error function. Note that there is no residue contribution from $\omega = 0$ to formula (C-8).

Combining (C-5) and (C-8), and ignoring the meaningless range $t \leq \rho/c$ where our approximations will not hold, we have

$$e_z^r(x,y;t) \approx \frac{\mu_0 I_0}{\pi} \left\{ \frac{1}{2\sqrt{t^2 - \rho^2/c^2}} + \frac{c\sqrt{t}}{\rho} \operatorname{Re} \left[-\frac{e^{-i\phi}}{(\pi t)^{1/2}} + \frac{c\sqrt{t}}{\rho} e^{-2i\phi} \left\{ 1 - w \left(\frac{i\rho e^{i\phi}}{2c\sqrt{t}t} \right) \right\} \right] \right\} \quad (t > \rho/c) \quad (C-9)$$

Using the small argument expansion for $w(z)$ given in ([25], p. 297, we have that

$$e_z^r(x,y;t) \sim \frac{\mu_0 I_0}{4\pi} \left\{ \frac{1}{t} + \frac{2}{3} \frac{\cos \phi}{c\sqrt{\pi T}} \frac{\cos \phi}{t^{3/2}} + o(t^{-2}) \right\} \quad (t \rightarrow \infty) \quad (C-10)$$

Note that this is the same asymptotic behavior that we found for the late-time portion e_{zd}^r of the solution in eqn. (B-8).

List of Figures

- Fig. 1: Pulsed line source above a conducting half-space: $x = \rho \cos \phi$, $y = \rho \sin \phi$.
- Fig. 2: Pulsed line source above an arbitrarily reflecting boundary.
- Fig. 3: Path of integration and singularities in the complex λ -plane for eqn. (6).
- Fig. 4: Cagniard contour $C(\phi)$ in the λ -plane; — path on proper sheet, - - - path on improper sheet.
- Fig. 5: Alternate choice of primary Riemann sheet convenient for Cagniard contour: $\text{Im}(u_1) \leq 0$.
- Fig. 6: Singularities of $\Gamma(\lambda, \omega)$ in λ -plane for a homogeneous, conducting half-space and ω real, positive. $\text{Im}(u_1, u_2) < 0$.
- Fig. 7: Same as Fig. 6, but $\omega = \omega_r + i\delta$, $\omega_r, \delta > 0$.
- Fig. 8: Extra branch cut integral required if $\epsilon_r < 1$ and $|\phi|$ sufficiently large.
- Fig. 9: Contours of integration in the λ -plane corresponding to eqn. (35): -----; and eqn. (38): _____.
- Fig. 10: Normalized reflected field $4\pi\rho e_z^r/\mu_0 I_0 c$ vs. normalized time t/T ; $\epsilon_r = 1$, $\rho/cT = 0.1$, $\phi = 88^\circ$. — exact, ——— quasistatic (eqn. (C-9)), very-long time approximation (eqn. (C-10)).
- Fig. 11: As in Fig. 10, but $\rho/cT = 1.0$.
- Fig. 12: As in Fig. 10, but $\rho/cT = 5.0$.
- Fig. 13: Normalized reflected field $4\pi\rho e_z^r/\mu_0 I_0 c$ vs. normalized time t/T ; $\epsilon_r = 4$, $\rho/cT = 1$, $\phi = 0^\circ$. — exact, - - - quasistatic (eqn. (C-9)), very-long time approximation (eqn. (C-10)), ——— short-time approximation (eqn. (34)).
- Fig. 14: As in Fig. 13, but $\phi = 45^\circ$.
- Fig. 15: As in Fig. 13, but $\phi = 75^\circ$.
- Fig. 16: As in Fig. 13, but $\phi = 80^\circ$.
- Fig. 17: As in Fig. 13, but $\phi = 89.99^\circ$.
- Fig. A.1 Branch cuts in complex ω -plane for $\Gamma_d(\lambda, \omega)$.
- Fig. C.1 Branch cuts for the functions (C-3) and (C-7) in the ω -plane.

List of Figures

- Fig. 1: Pulsed line source above a conducting half-space: $x = \rho \cos \phi$, $y = \rho \sin \phi$.
- Fig. 2: Pulsed line source above an arbitrarily reflecting boundary.
- Fig. 3: Path of integration and singularities in the complex λ -plane for eqn. (6).
- Fig. 4: Cagniard contour $C(\phi)$ in the λ -plane; — path on proper sheet, - - - path on improper sheet.
- Fig. 5: Alternate choice of primary Riemann sheet convenient for Cagniard contour: $\text{Im}(u_1) \leq 0$.
- Fig. 6: Singularities of $\Gamma(\lambda, \omega)$ in λ -plane for a homogeneous, conducting half-space and ω real, positive. $\text{Im}(u_1, u_2) < 0$.
- Fig. 7: Same as Fig. 6, but $\omega = \omega_r + i\delta$, $\omega_r, \delta > 0$.
- Fig. 8: Extra branch cut integral required if $\epsilon_r < 1$ and $|\phi|$ sufficiently large.
- Fig. 9: Contours of integration in the λ -plane corresponding to eqn. (35): -----; and eqn. (38): _____.
- Fig. 10: Normalized reflected field $4\pi\rho e_z^r/\mu_0 I_0 c$ vs. normalized time t/T ; $\epsilon_r = 1$, $\rho/cT = 0.1$, $\phi = 88^\circ$. — exact, ——— quasistatic (eqn. (C-9)), very-long time approximation (eqn. (C-10)).
- Fig. 11: As in Fig. 10, but $\rho/cT = 1.0$.
- Fig. 12: As in Fig. 10, but $\rho/cT = 5.0$.
- Fig. 13: Normalized reflected field $4\pi\rho e_z^r/\mu_0 I_0 c$ vs. normalized time t/T ; $\epsilon_r = 4$, $\rho/cT = 1$, $\phi = 0^\circ$. — exact, - - - quasistatic (eqn. (C-9)), very-long time approximation (eqn. (C-10)), ——— short-time approximation (eqn. (34)).
- Fig. 14: As in Fig. 13, but $\phi = 45^\circ$.
- Fig. 15: As in Fig. 13, but $\phi = 75^\circ$.
- Fig. 16: As in Fig. 13, but $\phi = 80^\circ$.
- Fig. 17: As in Fig. 13, but $\phi = 89.99^\circ$.
- Fig. A.1 Branch cuts in complex ω -plane for $\Gamma_d(\lambda, \omega)$.
- Fig. C.1 Branch cuts for the functions (C-3) and (C-7) in the ω -plane.

List of Figures

- Fig. 1: Pulsed line source above a conducting half-space: $x = \rho \cos \phi$, $y = \rho \sin \phi$.
- Fig. 2: Pulsed line source above an arbitrarily reflecting boundary.
- Fig. 3: Path of integration and singularities in the complex λ -plane for eqn. (6).
- Fig. 4: Cagniard contour $C(\phi)$ in the λ -plane; — path on proper sheet, - - - path on improper sheet.
- Fig. 5: Alternate choice of primary Riemann sheet convenient for Cagniard contour: $\text{Im}(u_1) \leq 0$.
- Fig. 6: Singularities of $\Gamma(\lambda, \omega)$ in λ -plane for a homogeneous, conducting half-space and ω real, positive. $\text{Im}(u_1, u_2) < 0$.
- Fig. 7: Same as Fig. 6, but $\omega = \omega_r + i\delta$, $\omega_r, \delta > 0$.
- Fig. 8: Extra branch cut integral required if $\epsilon_r < 1$ and $|\phi|$ sufficiently large.
- Fig. 9: Contours of integration in the λ -plane corresponding to eqn. (35): -----; and eqn. (38): ————.
- Fig. 10: Normalized reflected field $4\pi\rho e_z^r / \mu_0 I_0 c$ vs. normalized time t/T ; $\epsilon_r = 1$, $\rho/cT = 0.1$, $\phi = 88^\circ$. ——— exact, ——— quasistatic (eqn. (C-9)),, very-long time approximation (eqn. (C-10)).
- Fig. 11: As in Fig. 10, but $\rho/cT = 1.0$.
- Fig. 12: As in Fig. 10, but $\rho/cT = 5.0$.
- Fig. 13: Normalized reflected field $4\pi\rho e_z^r / \mu_0 I_0 c$ vs. normalized time t/T ; $\epsilon_r = 4$, $\rho/cT = 1$, $\phi = 0^\circ$. ——— exact, - - - quasistatic (eqn. (C-9)), very-long time approximation (eqn. (C-10)), ——— short-time approximation (eqn. (34)).
- Fig. 14: As in Fig. 13, but $\phi = 45^\circ$.
- Fig. 15: As in Fig. 13, but $\phi = 75^\circ$.
- Fig. 16: As in Fig. 13, but $\phi = 80^\circ$.
- Fig. 17: As in Fig. 13, but $\phi = 89.99^\circ$.
- Fig. A.1 Branch cuts in complex ω -plane for $\Gamma_d(\lambda, \omega)$.
- Fig. C.1 Branch cuts for the functions (C-3) and (C-7) in the ω -plane.

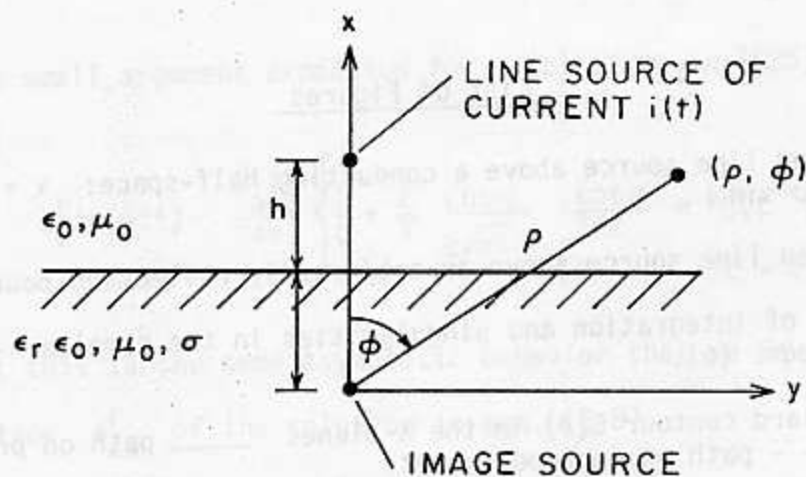


Figure 1

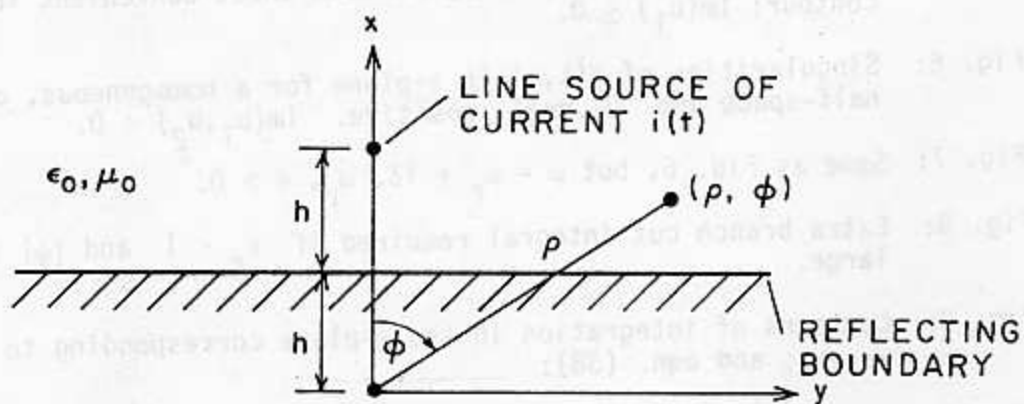


Figure 2

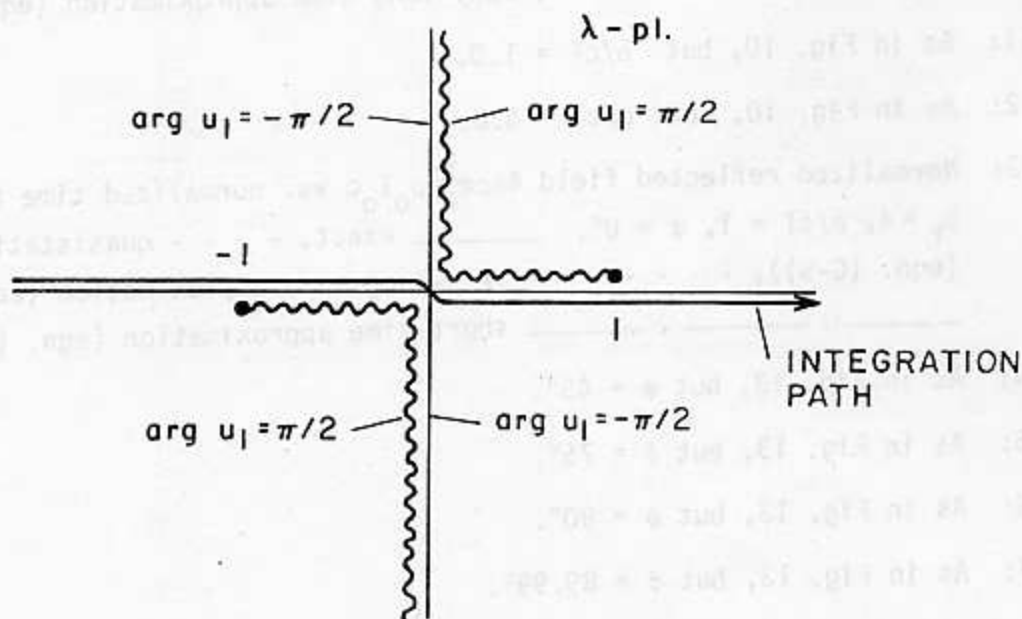


Figure 3

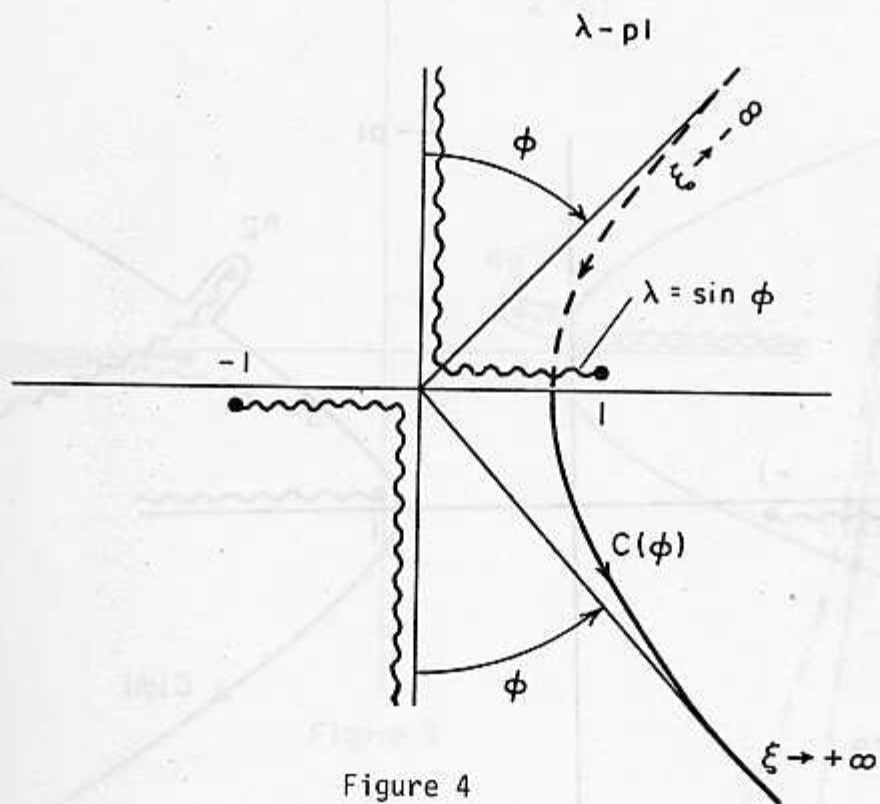


Figure 4

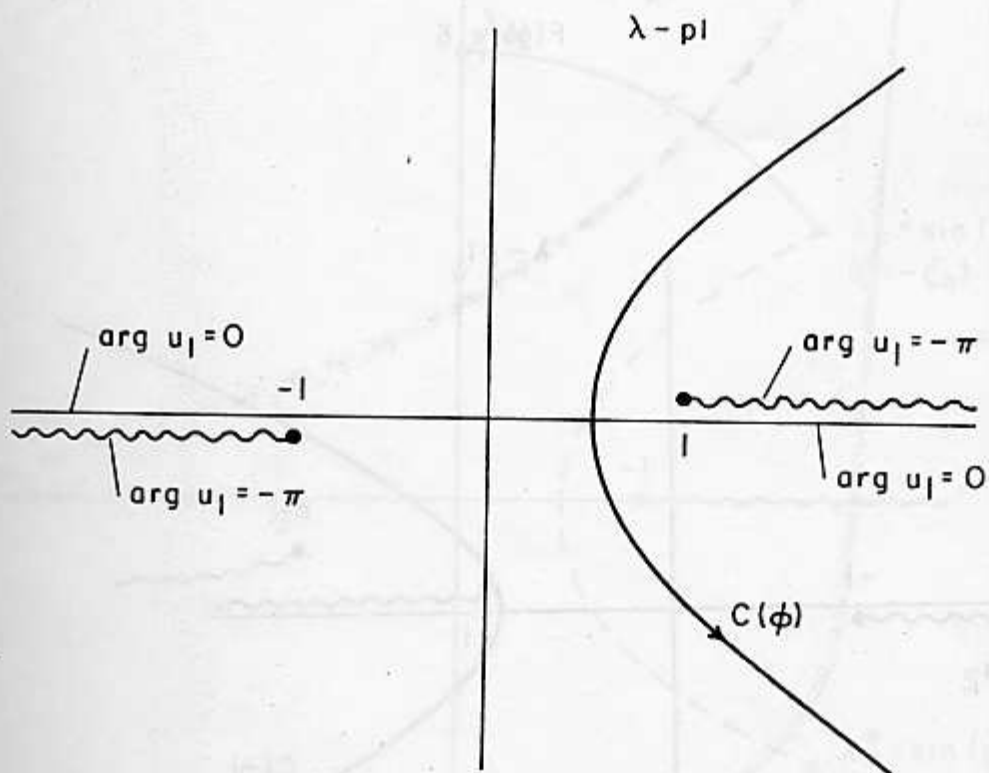


Figure 5

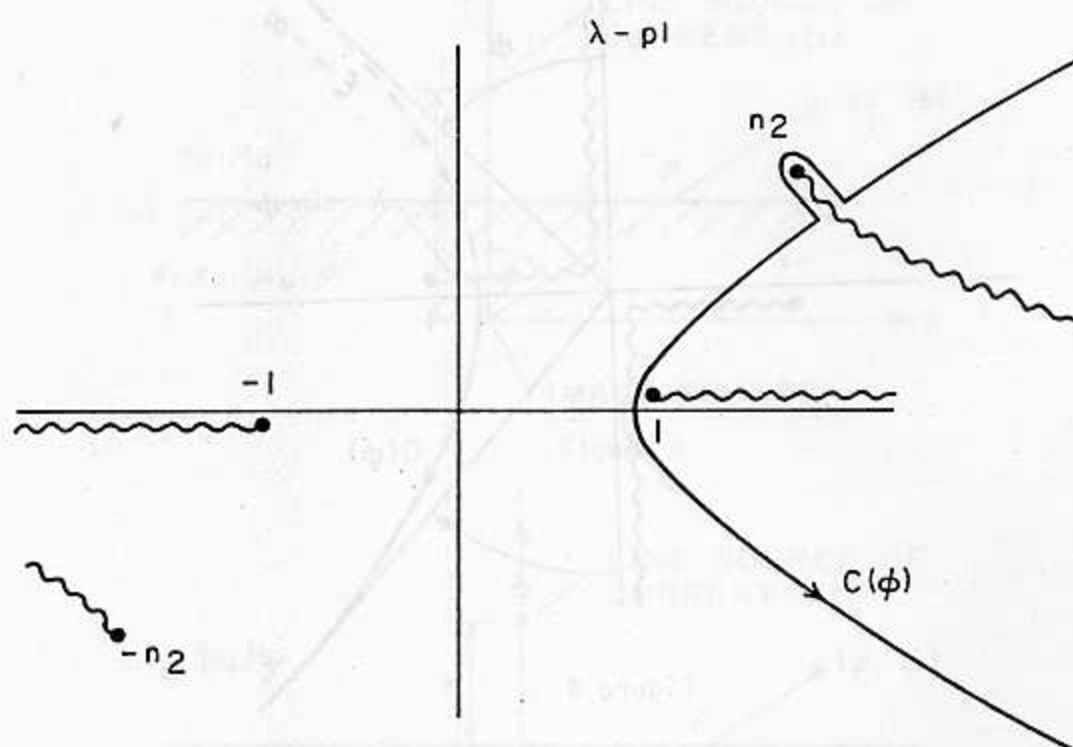


Figure 6

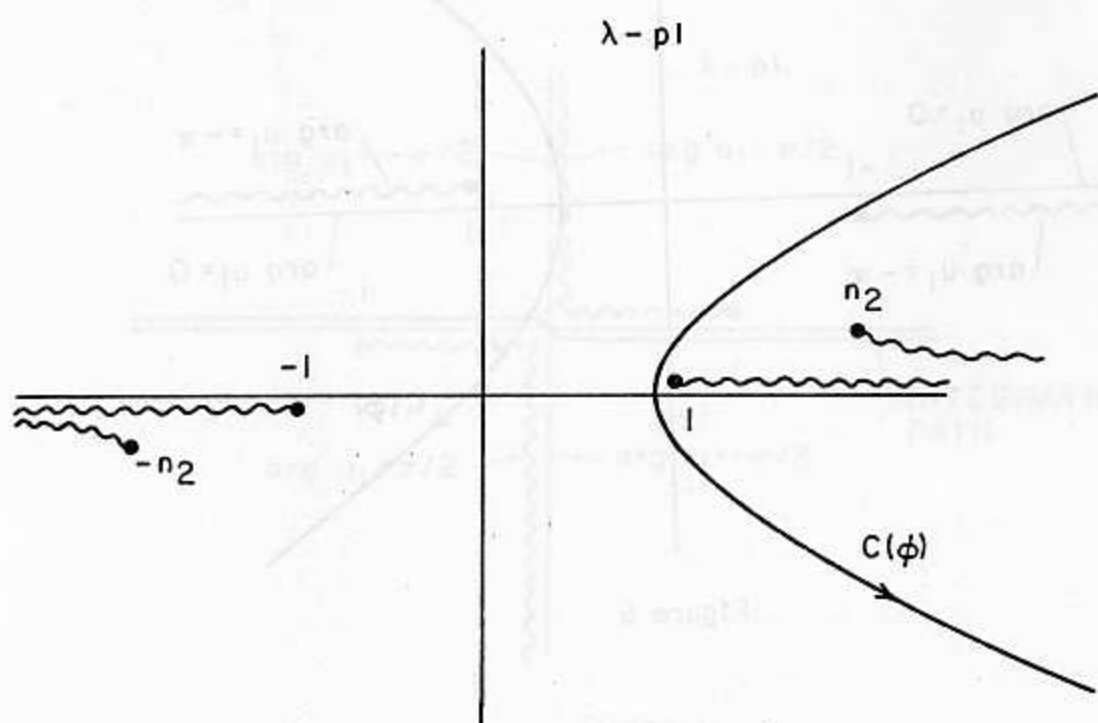


Figure 7

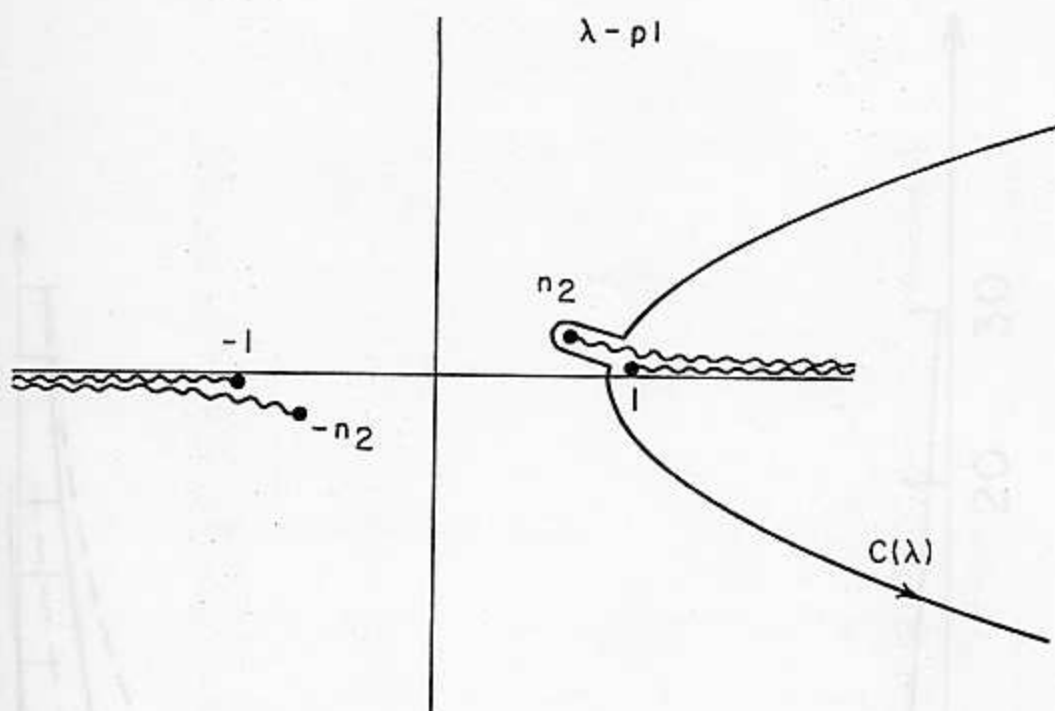


Figure 8

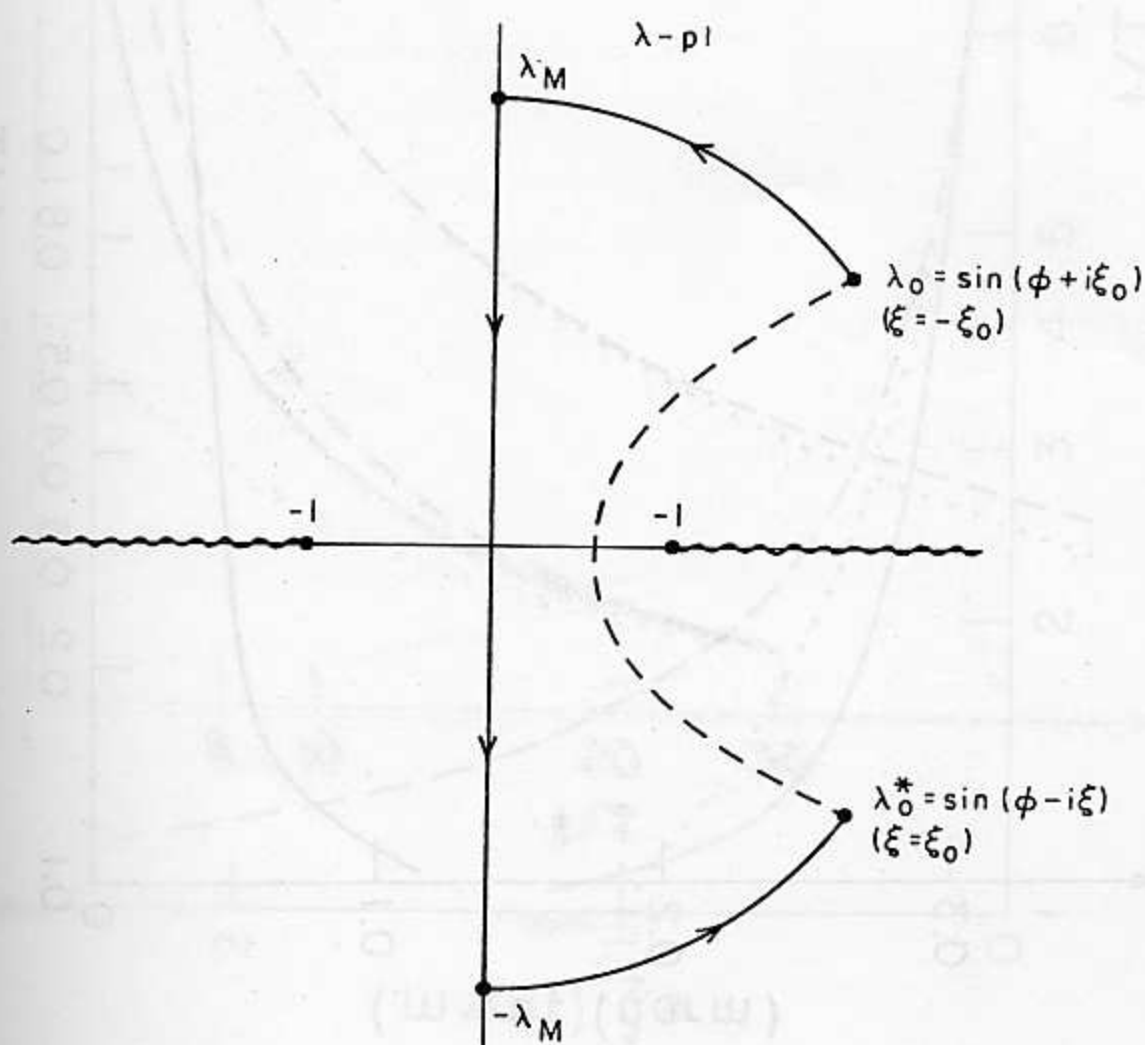


Figure 9

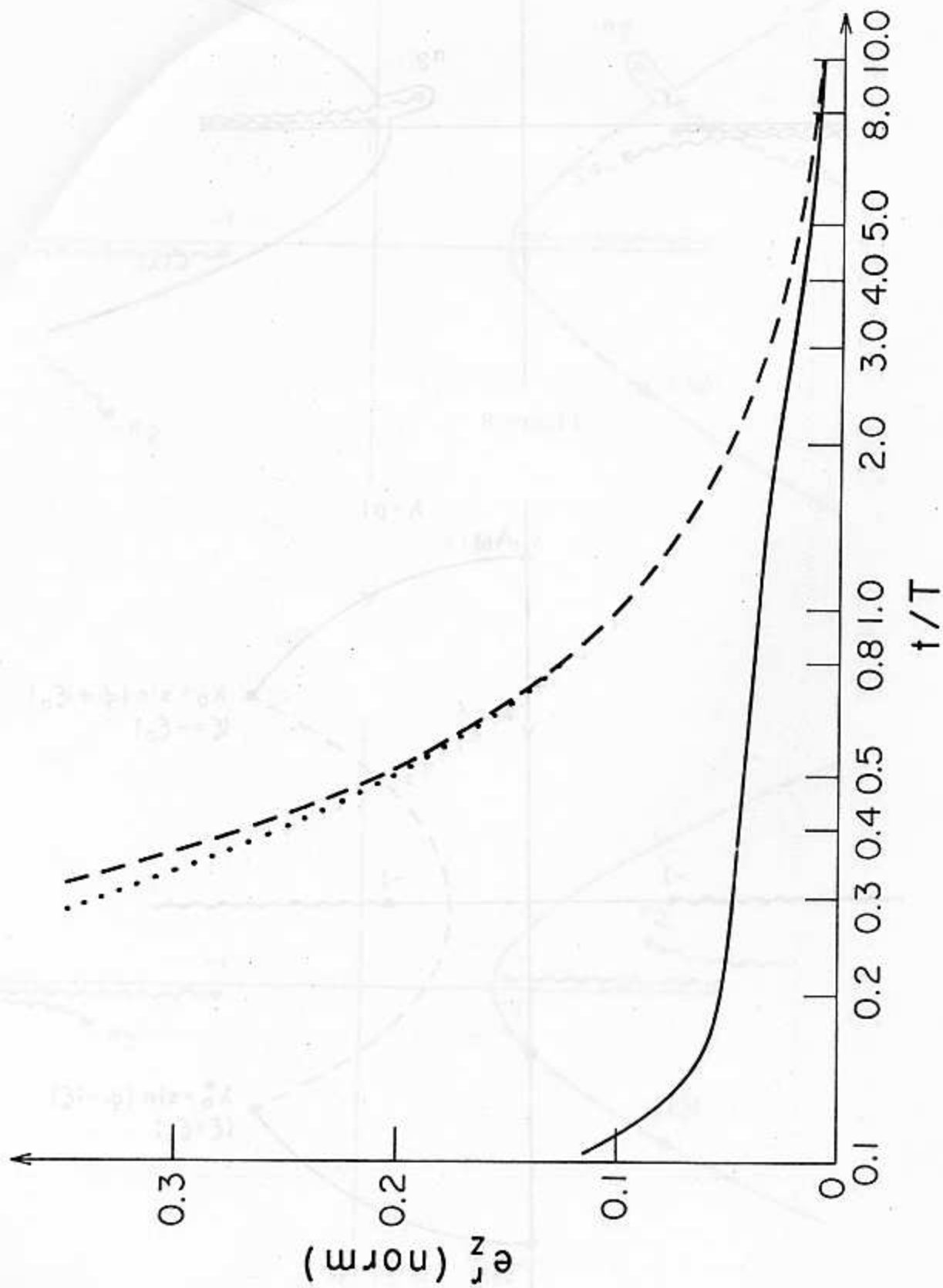


Figure 10

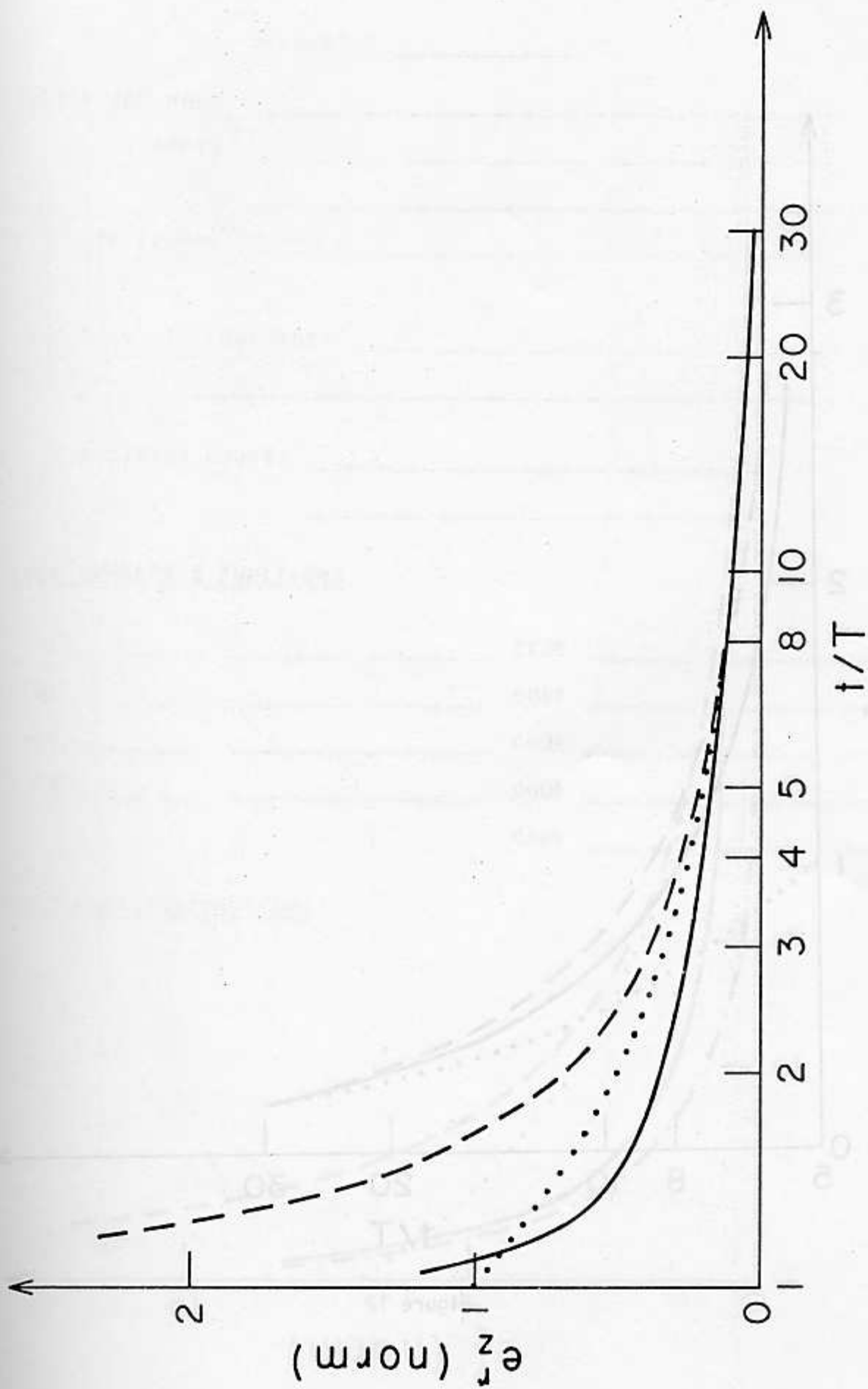


Figure 11

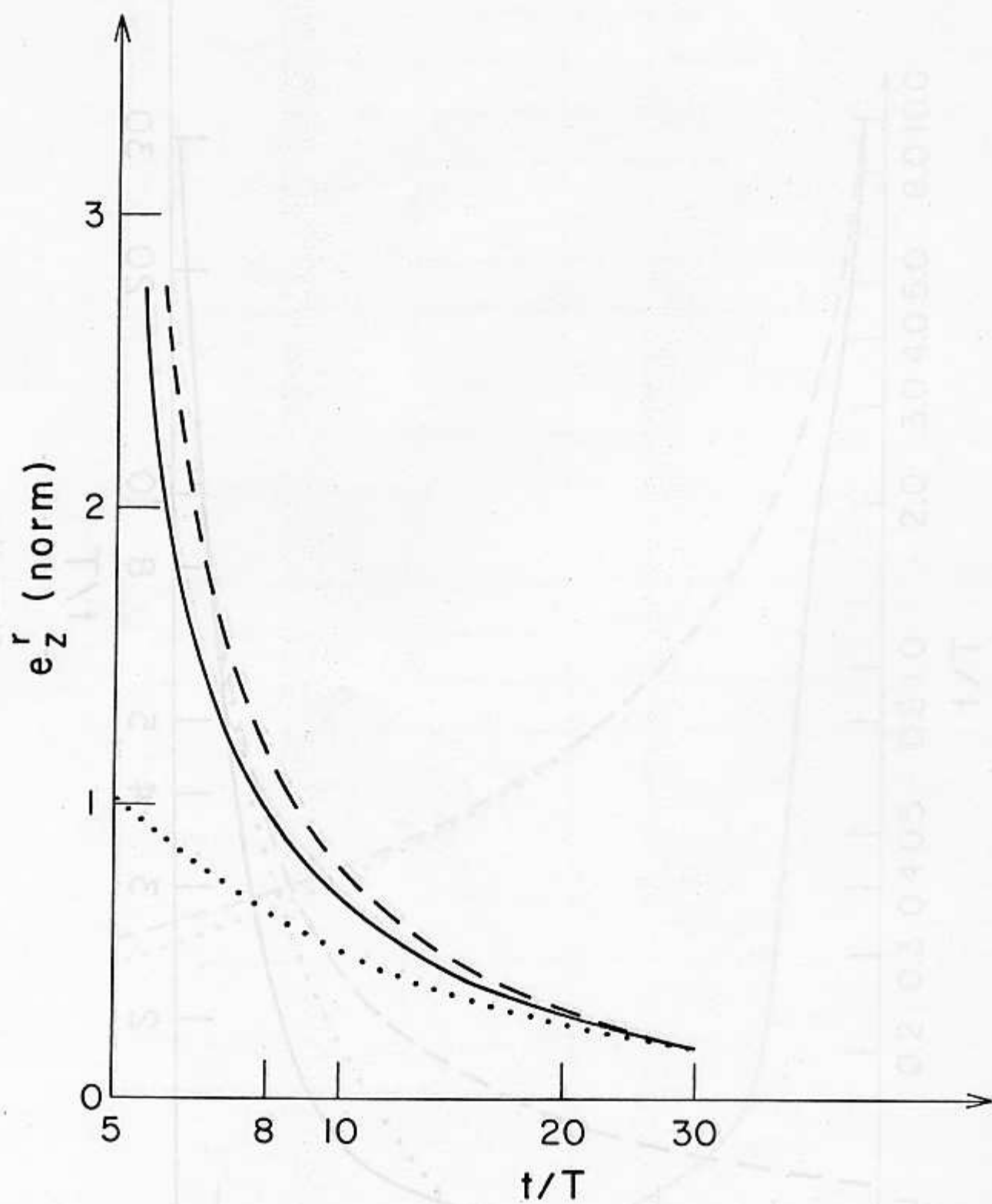


Figure 12

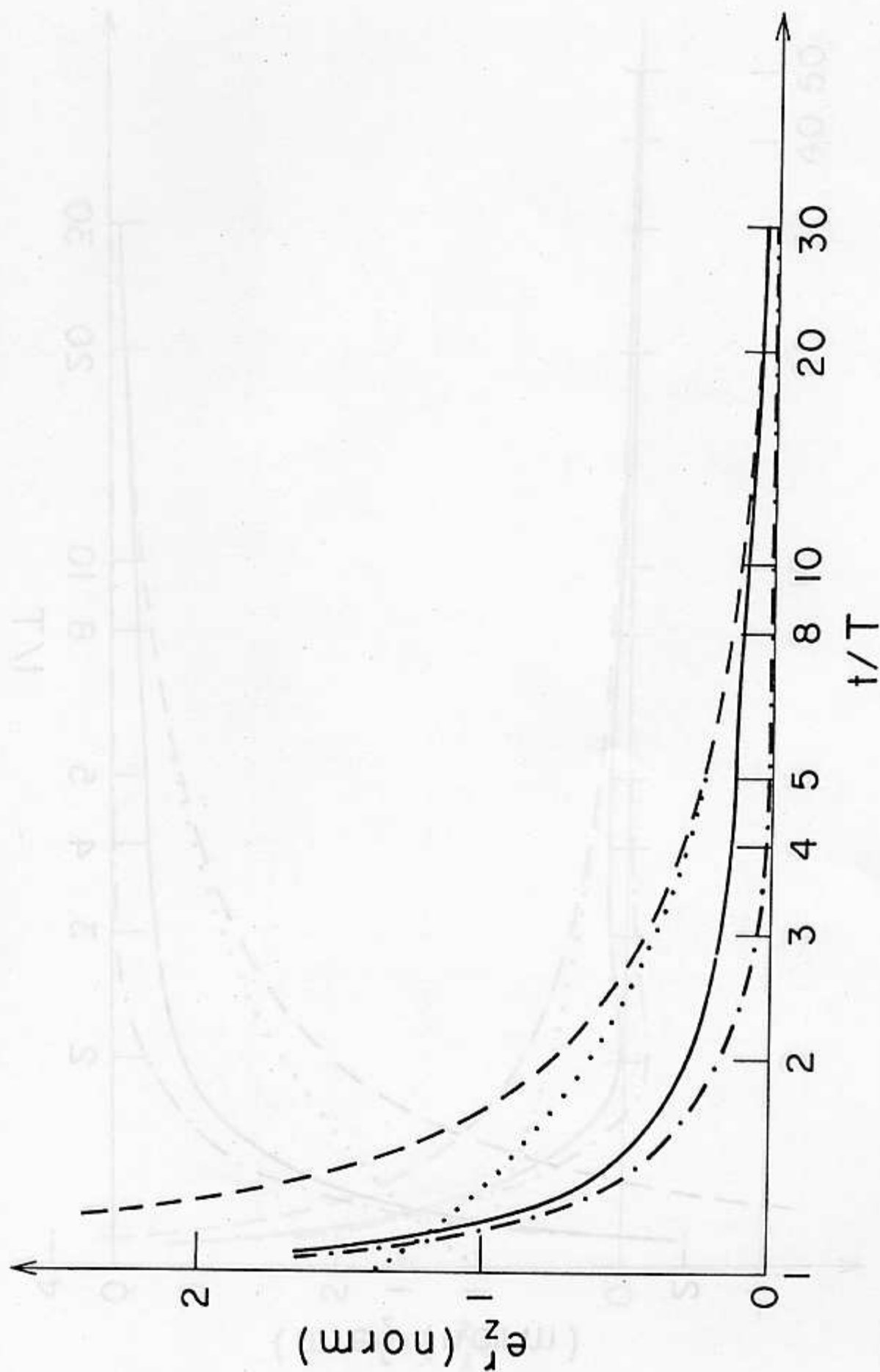


Figure 13

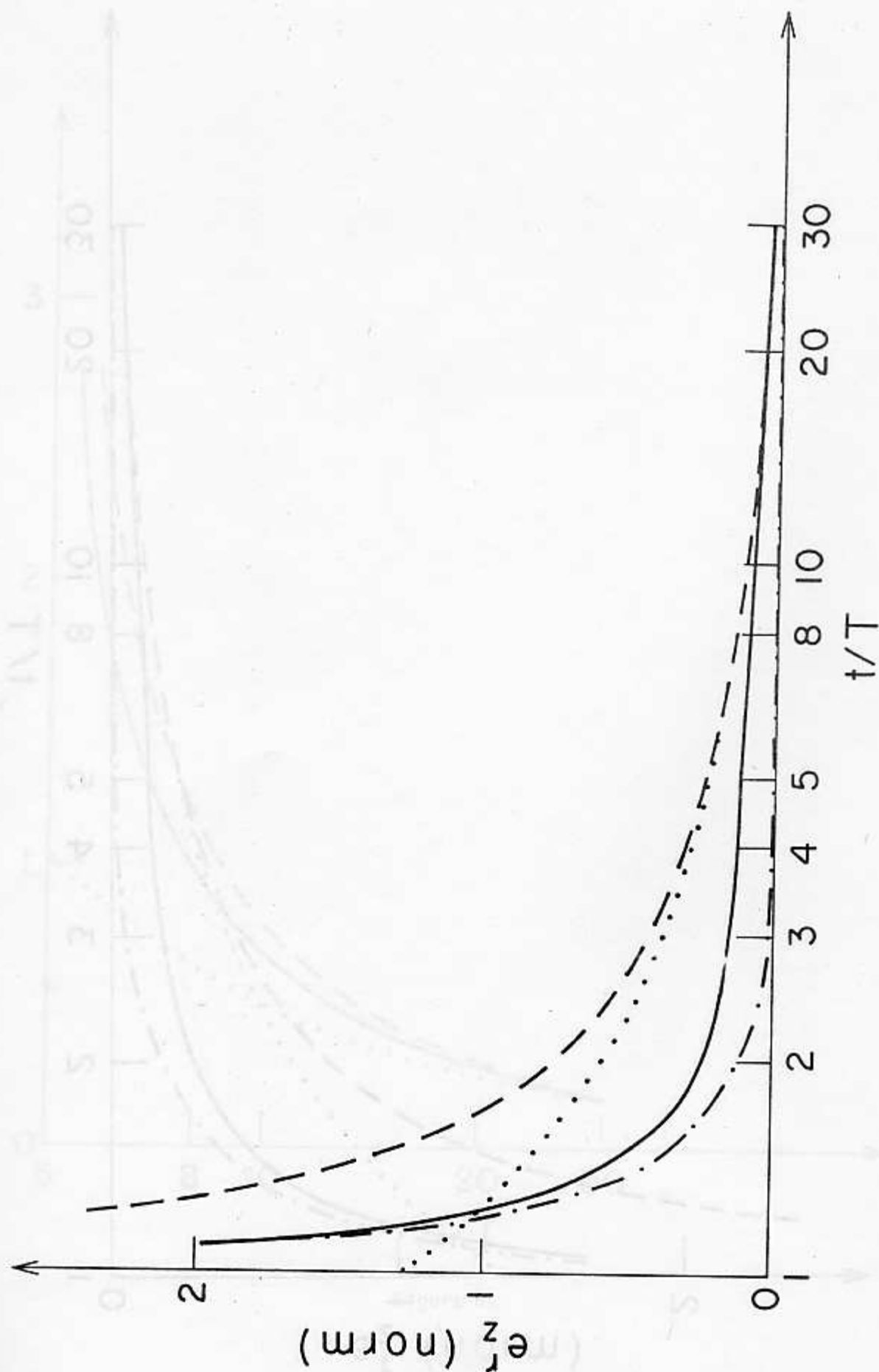


Figure 14

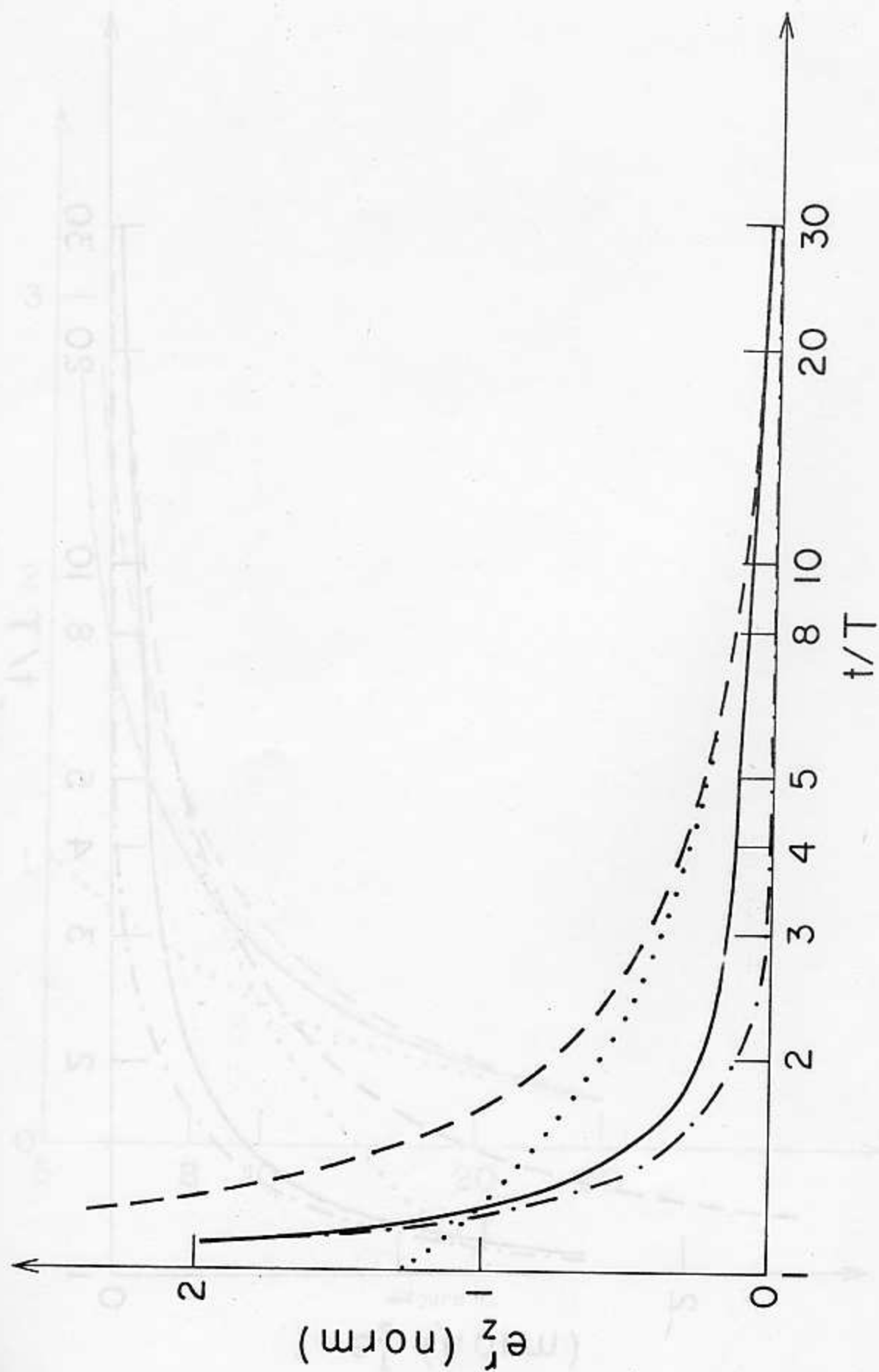


Figure 14

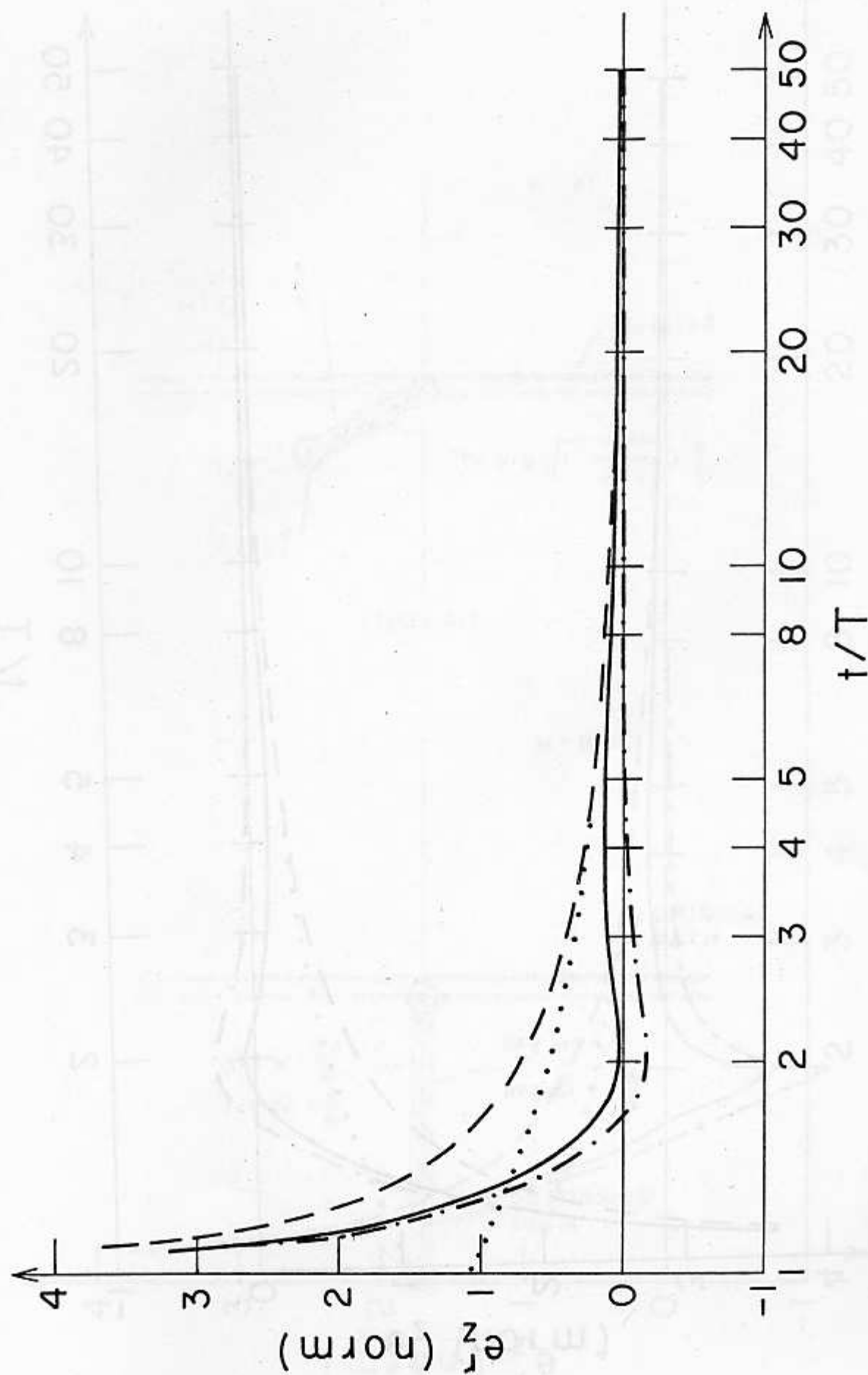


Figure 15

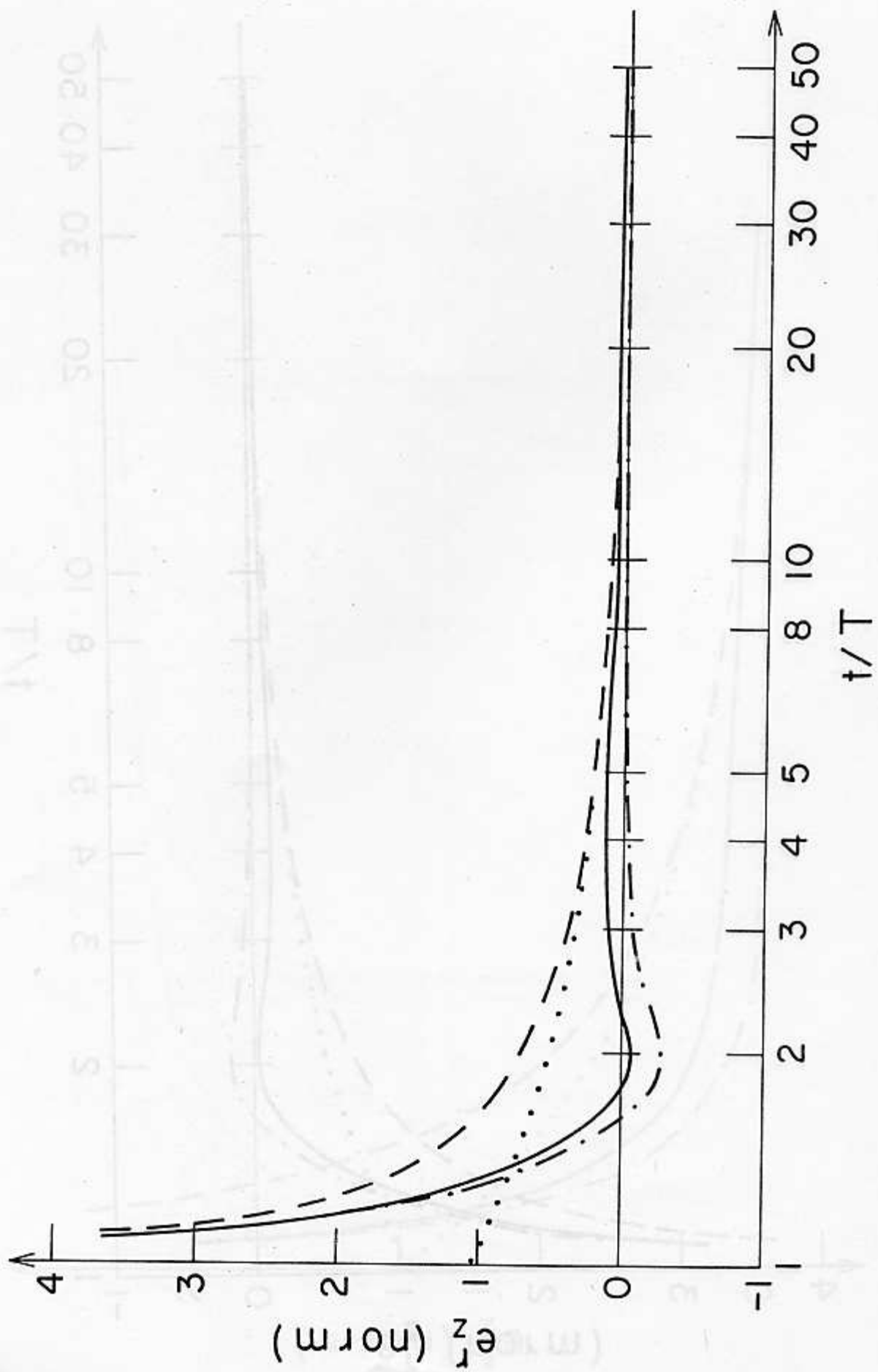


Figure 16

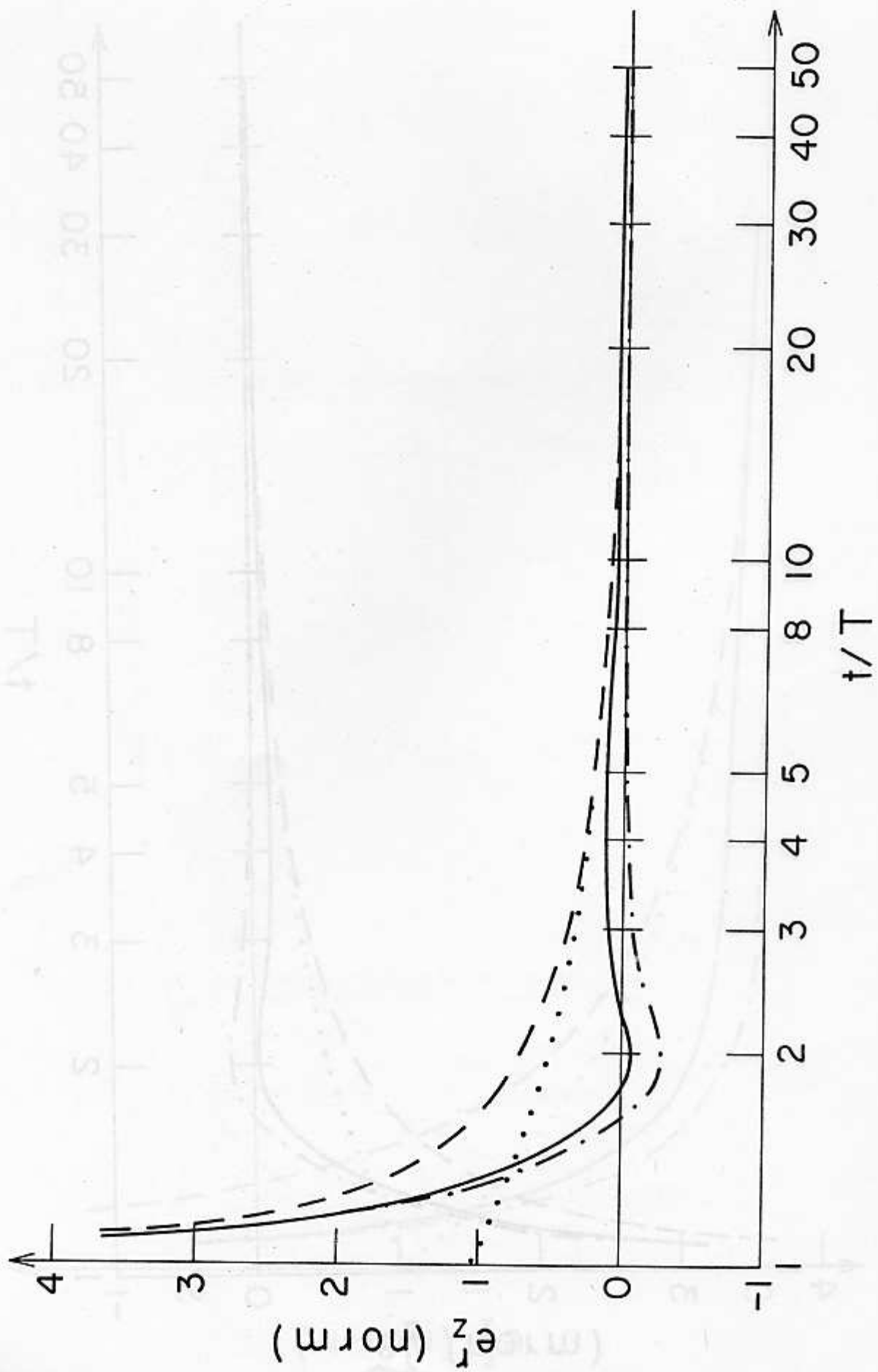


Figure 16

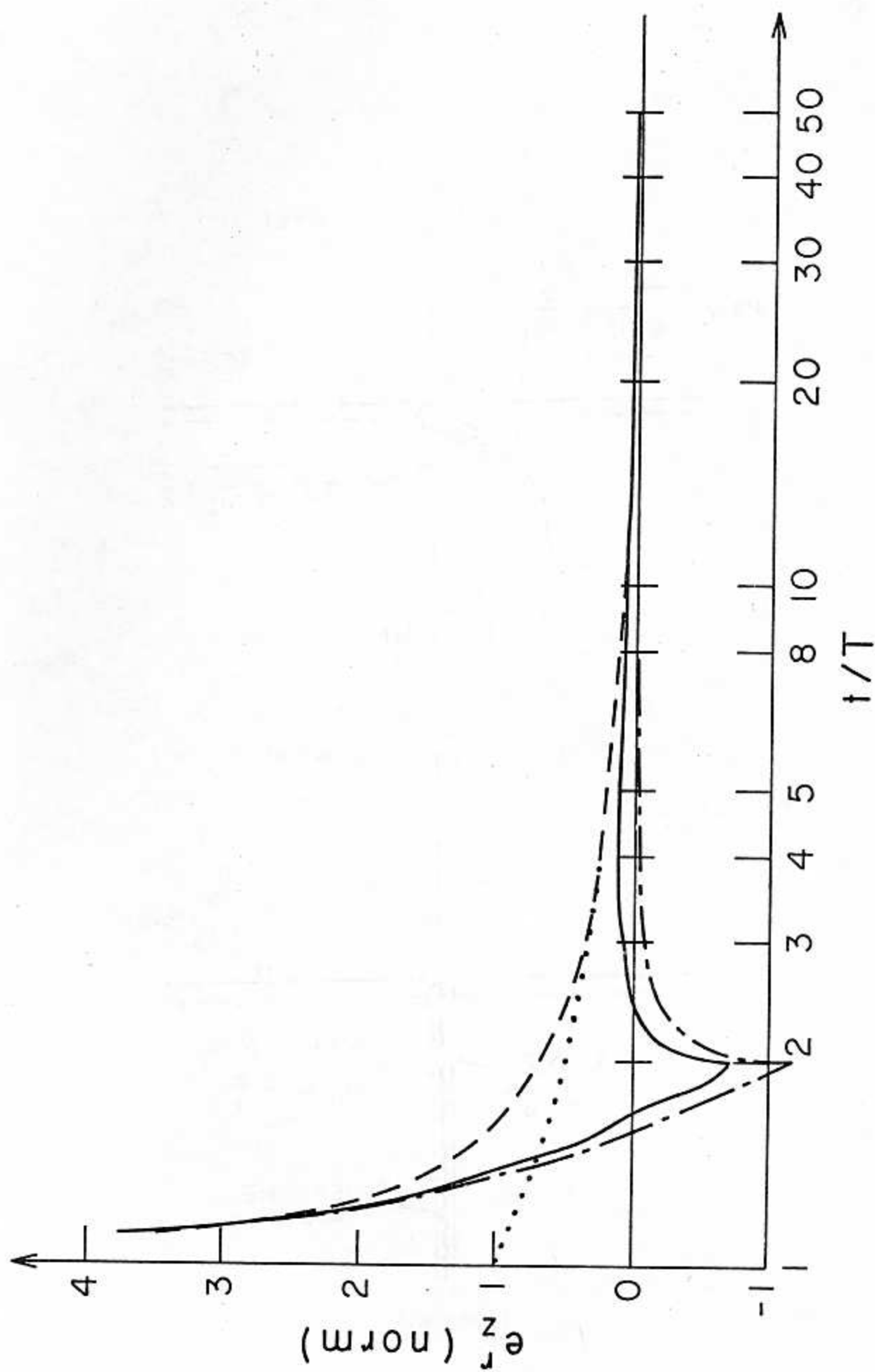


Figure 17

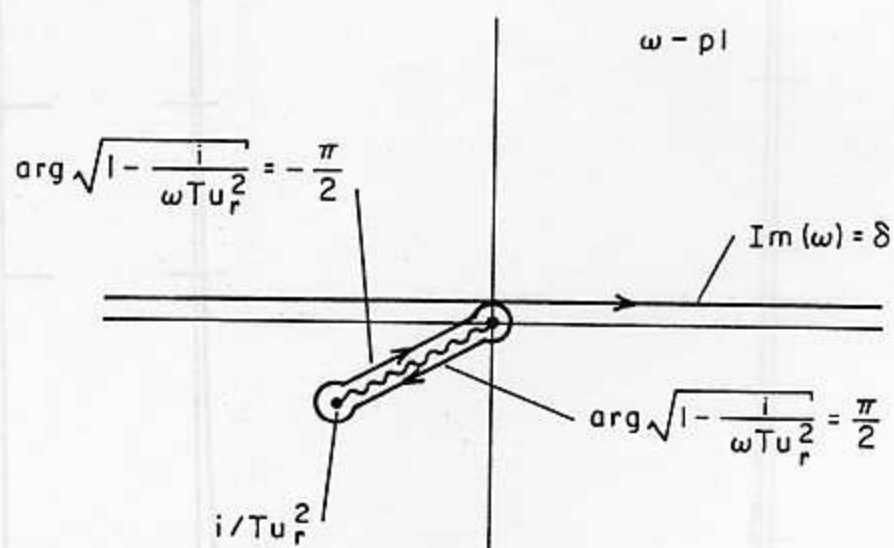


Figure A.1

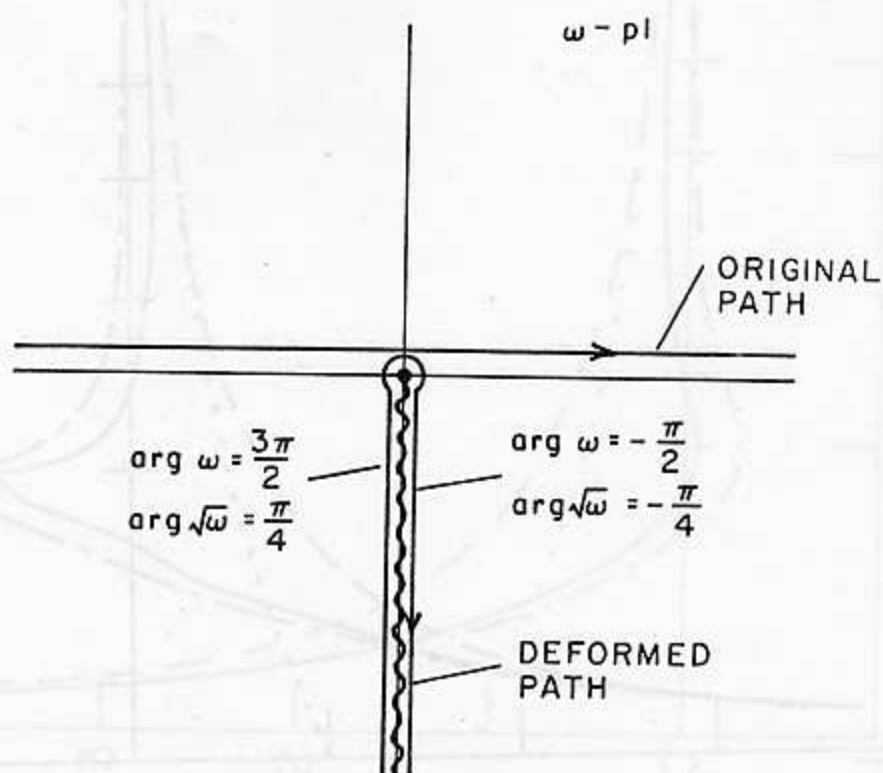


Figure C.1

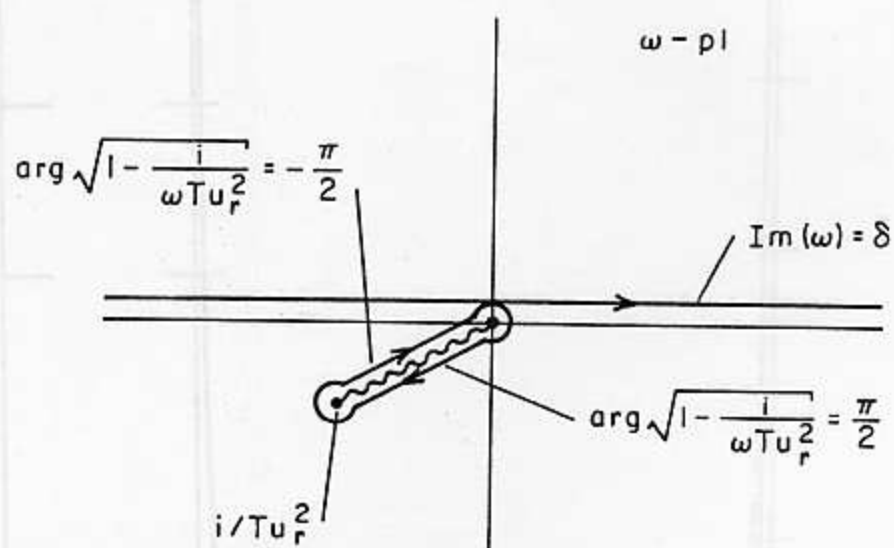


Figure A.1

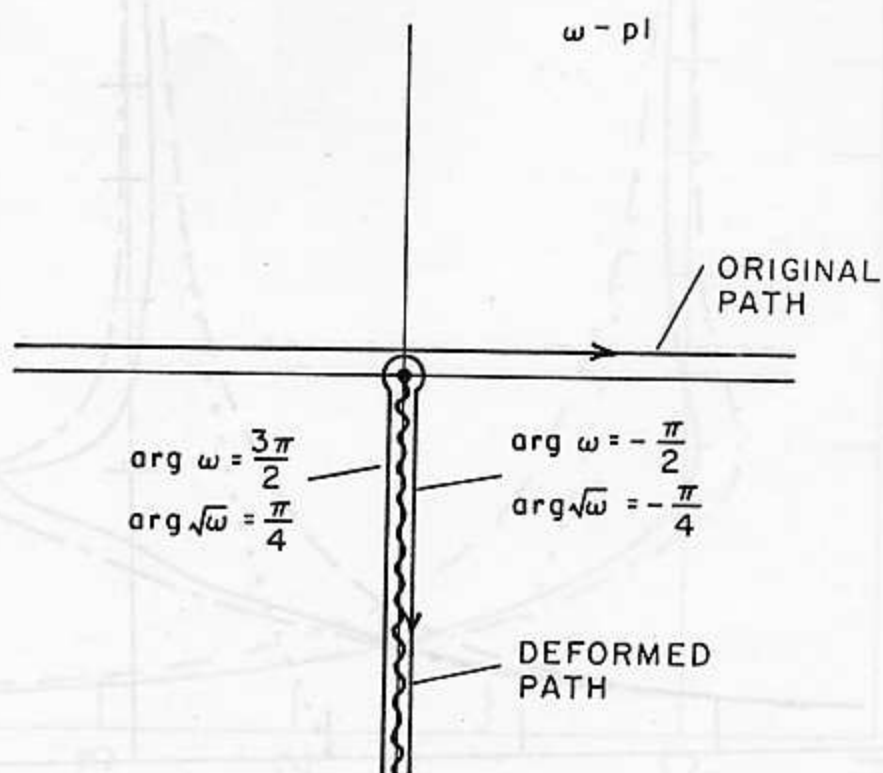


Figure C.1